

Chemistry and Engineering of Catalytic Hydrodesulfurization

G. C. A. SCHUIT and B. C. GATES

Department of Chemical Engineering
University of Delaware, Newark, Delaware 19711

SCOPE

The chemistry of catalytic hydrodesulfurization is not well understood although the hydrodesulfurization of petroleum distillates has been practiced industrially for years. The subject remains a neglected area of research, although there has been a recent surge in process development motivated by air pollution control standards requiring low sulfur fuel oils. The developments focus on processing of high-molecular-weight feeds, including residual oils. The results include large scale fixed- and fluidized-bed residuum hydrodesulfurization processes.

This review emphasizes the recent literature in summarizing the catalytic chemistry of hydrodesulfurization and identifying the process engineering problems.

The subject of reaction intermediates in hydrodesulfurization is reviewed thoroughly; kinetics for pure compounds and petroleum feedstocks are summarized; and structures of alumina-based catalysts (especially Ni/W and Co/Mo) are given in detail, leading to consideration of the catalytic sites.

The engineering literature of the new processes is sparse; consequently, the review is qualitative and speculative. The unique problems are related to plugging of catalyst pores by inorganic reaction products and to the possibility of unstable operation with exothermic reactions of explosive mixtures.

CONCLUSIONS AND SIGNIFICANCE

Reaction networks prevailing in catalytic hydrodesulfurization are known for only a few reactants, and results are not easily generalized; thiophene is desulfurized to butadiene before it is hydrogenated, but benzothiophenes are more rapidly hydrogenated than desulfurized. Rates of hydrodesulfurization vary greatly among feeds, being lowest for high-molecular-weight aromatic compounds like benzothiophene. Hydrodesulfurization of many reactants over a wide range of conditions is first order in reactant concentration and in hydrogen partial pressure; reaction is inhibited by product H_2S and by strongly adsorbed hydrocarbons.

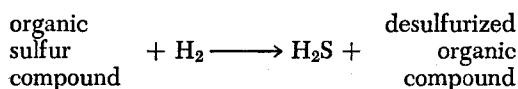
Catalysts have been described in terms of two models, the intercalated sulfide model in which the catalytic sites for hydrogenation and possibly hydrodesulfurization involve W^{3+} ions adjacent to vacancies at crystal edges and the monolayer model with catalytic sites involving Mo^{4+} ions octahedrally coordinated in a surface layer which is

stabilized by the presence of promoter Co^{2+} ions located in tetrahedral sites of the underlying support.

The processes for hydrodesulfurization of petroleum distillates are well established, and until recently there had been little incentive for improvement of catalysts. The more challenging problems of hydrodesulfurizing residual feeds stem from the lack of reactivity of the heavier sulfur compounds and the presence of organometallic feed components; these react to form inorganic products, which can permanently plug the pores of catalysts and contribute to plugging of the interstices of fixed-bed reactors. The catalyst aging phenomena have been countered by catalyst- and reactor-designs maximizing the capacity for unwanted products and optimizing their distribution. The deposited products influence flow distribution in reactors, and under some poorly defined circumstances the exothermic reactions may become uncontrollable and the operations hazardous.

GENERAL DESCRIPTION OF PROCESSES

Hydrodesulfurization reactions are those of the following class:



Correspondence concerning this paper should be addressed to B. C. Gates. G. C. A. Schuit is at the Technical University, Eindhoven, The Netherlands.

The literature of hydrodesulfurization chemistry and technology has been reviewed by McKinley (1957) and recently by Schuman and Shalit (1970), who included a thorough literature compilation.

Many light petroleum feedstocks have been treated with hydrogen in catalytic processes to remove sulfur. The light-feed desulfurization processes have had several objectives, among them pretreatment of catalytic reformer feeds to prevent poisoning of platinum catalyst by sulfur and treatment of gasoline formed in catalytic

cracking to provide sweetened and stabilized product.

Desulfurization of heavy petroleum fractions gives products including diesel and jet fuels, heating oils, and residual fuel oils. There is especially strong incentive for removal of sulfur from fuels, since combustion of sulfur-containing fuels is the primary cause of SO₂ pollution of the atmosphere; the pollution is most severe in the Eastern United States, Japan, and Western Europe.

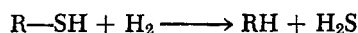
Feedstocks

In the following discussion we refer to light petroleum feeds, for which desulfurization technology is well established and routinely applied, and heavy feeds, including residual and perhaps gas oils, for which the relatively new technology is undergoing rapid evolution. Table 1 summarizes approximate boiling ranges of light and heavy feeds used in hydrosulfurization processes.

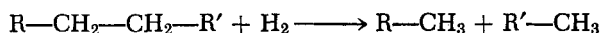
Petroleum feedstocks include the sulfur-containing compounds listed in Table 2. The compound classes are listed in order of generally decreasing reactivity in hydrosulfurization: thiols are very reactive, and thiophenes are much less reactive. The kinetics and reaction networks in hydrosulfurization are to be discussed in detail later.

Reactions

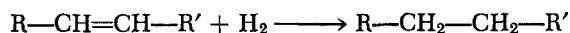
The following is a preliminary listing of the important reactions occurring in hydrosulfurization processes, including side reactions which influence process design. Among those taking place in hydrosulfurization reaction networks are hydrogenolysis reactions which result in cleavage of a C—S bond. For example,



Under industrial reaction conditions hydrogenolysis reactions which result in breaking of C—C bonds also occur. The following hydrocracking reaction is an example:



Hydrogenation of unsaturated compounds also occurs:



These latter two classes or reactions take on importance by consuming hydrogen in the process without removing sulfur. Cracking reactions can also take place to produce molecular weight reduction.

Demetallization (or demetallation) reactions are important in hydrosulfurization of residual feeds. The heaviest fractions of some petroleum feedstocks contain significant concentrations of organometallic compounds, especially of V and Ni. The organometallic compounds react to give inorganic products, which can accumulate in a reactor and ultimately plug the pores of a catalyst or the interstices of a fixed bed of catalyst particles.

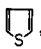

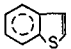
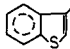
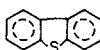
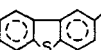
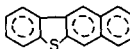
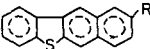
Coking reactions, common to virtually all hydrocarbon reaction processes, occur as well in hydrosulfurization. Coke is high-molecular-weight, hydrogen-deficient hydrocarbon product which poisons catalysts and is capable of blocking catalyst pores or fixed bed interstices. Unlike inorganic compounds of V, for example, coke can be burned off catalysts (as in catalytic cracking processes), leading to successful regeneration.

The hydrosulfurization reactions, which dominate over side reactions in industrial processes, are virtually irreversible at temperatures and pressures ordinarily applied, roughly 600 to 750°K and up to 2×10^7 N/m² (about 3,000 lb./sq.in.). The hydrosulfurization reactions are exothermic with heats of reaction of the order of

TABLE 1. PETROLEUM FRACTIONS

Petroleum feedstock	Approximate boiling range, °K
"light"	Light gasoline C ₄ -350
	Naphtha (reformer feed) 350-430
	Kerosene (jet fuel) 420-500
"heavy"	Gas Oil (diesel and heating oil) 440-640
	Residual oil (fuel oil) >620

TABLE 2. SOME SULFUR-CONTAINING COMPOUNDS IN PETROLEUM

Compound Class	Structures
Thiols (Mercaptans)	R-SH
Disulfides	R-S-S-R'
Sulfides	R-S-R'
Thiophenes	 ,  , etc.
Benzothiophenes	 ,  , etc.
Dibenzothiophenes	 ,  , etc.
Benzonaphthothiophenes	 ,  , etc.

5 to 9×10^4 J/mole hydrogen consumed (about 50 to 100 B.t.u./std.cu.ft. hydrogen consumed).

Catalysts

The catalysts most commonly applied in hydrosulfurization are derived from alumina-supported oxides of cobalt and molybdenum, which are usually sulfided in operation. Catalysts of this type are commonly referred to as cobalt molybdate. Practical catalysts may contain as much 10 to 20% of these metals, though lower metal contents are probably more common. A number of related compositions have been applied, including, for example, Ni and W. In contrast to the supported Pt and Pt-alloy catalysts used in reforming, the hydrosulfurization catalysts have hydrogenation activity in the presence of high concentrations of sulfur compounds.

The catalysts are used as porous pellets or extrudates, typically having dimensions of 1.6 to 3.2×10^{-3} m. The particle size and pore geometry have an important influence on process design (especially for the heaviest feeds) since intraparticle mass transport has a significant influence on reaction rates.

Detailed discussion of the bulk and surface structures of some hydrosulfurization catalysts will follow, as will analysis of the effects of mass transport on process design.

Reactors and Processing Conditions

Hydrogen and gas- or liquid-phase petroleum are contacted with solid catalyst in a fixed- or fluidized-bed reactor. Light feeds are invariably processed in a fixed bed, and the reactor design is straightforward and often based on plant operation. Hydrogen and petroleum in the vapor and/or liquid state flow cocurrently downward through a bed of catalyst particles. A simplified process flow diagram is shown in Figure 1. Hydrogen from the product stream is recycled and scrubbed; hydrogen flow

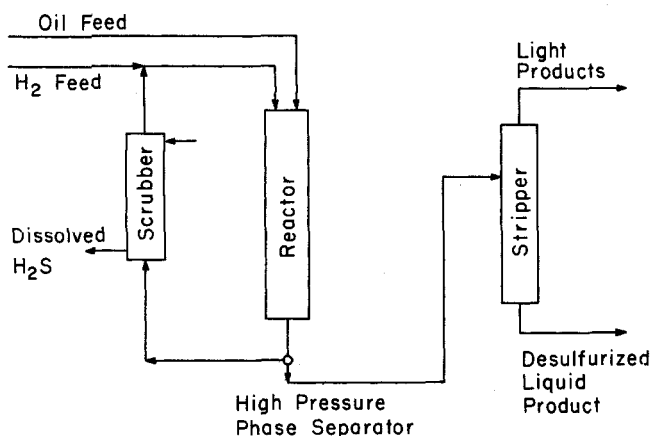


Fig. 1. Simplified diagram of hydrodesulfurization process.

rates may be 50 to 250 std. m^3/m^3 petroleum. The oil flows in a single pass through the reactor at space velocities depending on temperature, pressure, and the degree of desulfurization required; values of space velocity of 5.25×10^{-4} V/V/sec. (volumes of liquid oil at standard conditions per volume of packed bed reactor per second) may be considered representative of light feeds. Pressures are usually of the order of 10^6 N/m 2 , but may occasionally be as much as 10^7 N/m 2 . A typical operating range is approximately 575 to 675°K; temperature is usually increased gradually to compensate for activity decline caused by coke accumulation. Coke is periodically burned off the catalyst, which may have a lifetime of several years or more. In hydrodesulfurization of light feeds, catalyst costs typically account for less than about 10% of processing costs, and there is therefore not great incentive for developing new catalysts; it seems unlikely that there will soon be significant changes in processing technology.

If the reacting petroleum is liquid, then the reactor is a gas-liquid-solid reactor, referred to as a trickle-bed reactor. Hydrodesulfurization processes appear to be the most important applications of this reactor type (Satterfield, 1970).

Trickle-bed reactors are also used on an industrial scale in hydrodesulfurization of residual feeds. Operating conditions are more severe with these less reactive feeds. For example, temperatures may be 625 to 725°K; pressures 3 to 20×10^6 N/m 2 ; space velocities 1.5 to 6×10^{-4} V/V/sec.; and hydrogen recycle rates 300 to 1500 std. m^3/m^3 petroleum. The previously mentioned side reactions become important, especially at the highest temperatures. Deposits of coke and inorganic metal compounds are more readily formed with these heavy feeds. Large amounts of the deposited metals prevent regeneration of catalysts; in the application of nonregenerable catalysts, the residuum hydrodesulfurization process may be unique among large-scale catalytic processes involving hydrocarbons.

The problems of catalyst aging set heavy feed processes apart from the others. The associated processing problems will be discussed in detail later with other engineering aspects, for example, the problems of obtaining efficient fluid-solid contacting, uniform catalyst bed temperatures, and efficient catalyst utilization in the presence of significant mass transport resistances.

Another gas-liquid-solid reactor used commercially in residuum hydrodesulfurization is the slurry-bed reactor (Satterfield, 1970). This is also referred to as an *ebullating-bed* or *fluidized-bed* reactor since the catalyst particles

are held in suspension by the upward velocity of the liquid reactant through which hydrogen flows cocurrently. There are several advantages to this reactor design: (1) The deactivating catalyst can be removed and replaced continuously (as in catalytic cracking); (2) Small particles of catalyst can be used, and these are more effective than large particles when intraparticle mass transport resistance is significant (particles with a dimension less than about 1.6×10^{-3} m are avoided in fixed beds because pressure drops are unacceptably high); and (3) The fluidized bed reactor contents are expected to be very well mixed, which suggests that uniform temperatures can be maintained.

There are compensating disadvantages to the slurry-bed reactor: (1) The high degree of mixing of reactants in the direction of flow necessitates higher temperatures or lower space velocities than in a fixed bed to achieve the same conversion; (2) Corresponding to higher operating temperatures, undesired side reactions are more important, leading to higher hydrogen consumptions; (3) It is not clear that problems of reactor stability and control have been solved for the fluidized system with exothermic reactions involving hydrogen at high temperatures and pressures.

CATALYTIC CHEMISTRY

Reactions

Petroleum contains many different compounds susceptible to hydrodesulfurization. Sulfur may be bonded to one carbon, as in thiols and disulfides; to two carbons of alkyl groups, as in sulfides; or to two carbons of aromatic groups, as in thiophene and dibenzothiophene. Some basic questions concerning hydrodesulfurization reactions are these:

1. What stable intermediates are formed in hydrodesulfurization of these compounds, that is, what are the reaction networks?
2. What are the relative reactivities of the various classes of sulfur-containing compounds? Can effects of substituent groups on reactivities within a given class be described concisely?
3. Are the reaction networks and supposed generalizations about reactivities valid for broad groups of hydrodesulfurization catalysts?
4. What surface intermediates can be inferred from reaction chemistry and structures of catalysts?

The literature provides incomplete answers to these questions as discussed in the following sections.

Reaction Networks. Thiophenes are the least reactive sulfur compounds in petroleum; consequently, the simplest and most easily obtained compound in this class, thiophene itself, has been chosen frequently for study, being regarded as an appropriate model reactant. Thiophene hydrodesulfurization was examined in a thorough set of kinetic studies by Amberg and coworkers (Owens and Amberg, 1961, 1962; Desikan and Amberg, 1963, 1964; Kolboe and Amberg, 1966). The catalysts were a commercial cobalt molybdate (1.3% Co and 6.1% Mo), chromia, and several molybdenum disulfides. Kinetic data were obtained from a pulse microreactor and from a steady state flow reactor operated at low conversions (<0.5%). Reaction products were included in feeds to provide identification of reaction inhibitors and intermediates in reaction networks. Some conversion and product distribution data from the steady state flow reactor study of Kolboe and Amberg (1966) are collected in Tables 3 and 4.

Owens and Amberg (1961) also used the microreactor containing chromia catalyst for determination of conversions of the individual compounds listed in Table 5. The data of Tables 4 and 5 lead to the reaction network suggested in Figure 2 for thiophene hydrodesulfurization catalyzed by chromia and by cobalt molybdate.

The suggestion that the first reaction of thiophene in the primary reaction path is the C—S bond cleavage to

TABLE 3. CATALYST ACTIVITIES IN THIOPHENE HYDRODESULFURIZATION (KOLBOE AND AMBERG, 1966)

Catalyst	$10^{-3} \times \text{BET area, m}^2/\text{kg}$	Apparent reaction rate ^{a,b} , (moles/sec. m ²)
MoS ₂	3.3	0.9
MoS ₂ + 1% Co	3.3	0.5
MoS ₂ from MoS ₃ heated to 673°K	154	11.0
MoS ₂ from MoS ₃ heated to 923°K	67	1.6
MoS ₂ from MoS ₃ heated to 1073°K	12	1.5
Cobalt molybdate	241	1.6
Cr ₂ O ₃	150	2.0

^a Rate of reaction varied significantly between fractional conversions of zero and 0.005. Tabulated values are average rates between these two conversions.

^b Data were obtained in a steady state flow reactor at 561°K. Partial pressures of hydrogen and thiophene were 1.00×10^6 and 2.7×10^3 N/m², respectively. Flow rate of hydrogen was maintained at about 3×10^{-7} m³/sec. Amounts of catalyst were varied to give a surface area of 2-5 m² for each.

form 1,3-butadiene, rather than hydrogenation of the C=C bond, is supported by further data of Desikan and Amberg (1964). Their results show that the hydrogenated compound with the C—S bonds intact (tetrahydrothiophene) gives products in hydrodesulfurization different from those observed for thiophene. The result that the C—S bonds in thiophene are broken before hydrogenation of double bonds is contrary to first expectations—since the aromatic compounds are so unreactive, one might expect that the saturated compound would be formed, which could then be desulfurized rapidly.

Amberg and coworkers also observed that H₂S inhibited

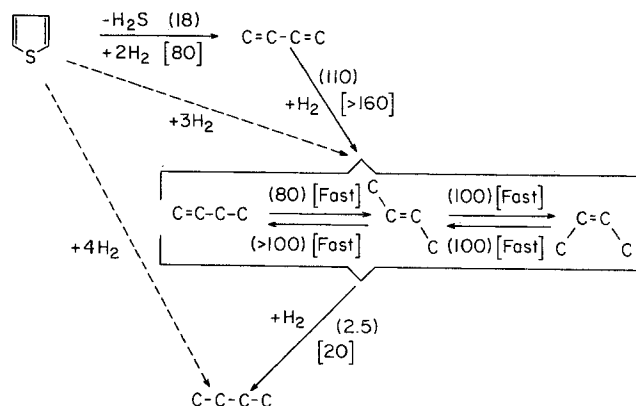


Fig. 2. Thiophene hydrodesulfurization reaction network. Numbers in parentheses are approximate rates (nmole)/kg/sec.) with chromia catalyst at 688°K; numbers in brackets for cobalt molybdate catalyst at 673°K (Owens and Amberg, 1961).

TABLE 4. PRODUCT DISTRIBUTION IN THIOPHENE HYDRODESULFURIZATION (KOLBOE AND AMBERG, 1966)

Catalyst	Butadiene	Mole % in C ₄ Hydrocarbon Product				Butane
		1-Butene	cis-2-butene	trans-2-butene		
MoS ₂	6.9	42.5	22.3	19.2		8.8
MoS ₂ + 1% Co	8.4	55.6	14.0	17.4		4.7
MoS ₂ from MoS ₃ heated to 673°K	7.2	39.9	16.7	23.5		12.7
MoS ₂ from MoS ₃ heated to 923°K	4.0	28.5	22.0	36.5		9.5
Cobalt molybdate	2.2	47.5	19.8	24.3		6.2
Cr ₂ O ₃	7.7	31.3	11.8	11.8		37.4

Products from steady state flow reactor at 0.5% conversion of thiophene. Other conditions are specified in Table 3.

TABLE 5. PRODUCT DISTRIBUTION IN REACTIONS CATALYZED BY CHROMIA (OWENS AND AMBERG, 1961)

Reactant	Isobutane	n-Butane	Mole % in C ₄ Hydrocarbon Product			cis-2-butene + butadiene
			1-Butene + isobutene ^a	trans-2-butene		
Thiophene	0.0	8.6	30.1	27.4		33.9 ^b
1,3-Butadiene	0.0	2.0	23.1	36.7		38.2 ^b
1-Butene	0.0	8.9 ^c	42.1	26.6		22.4
trans-2-Butene	0.0	1.9	22.3	52.4		23.5
cis-2-Butene	0.0	2.0	21.2	37.6		39.2
Isobutene	2.0	0.0	98.0	0.0		0.0
n-Butane	—	100.0	0.0	0.0		0.0
n-Butenes ^d	—	—	20	48		32

Conversions in a pulse microreactor at 688°K.

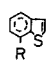
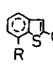
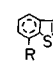
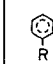

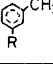
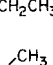
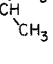
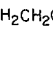

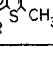
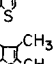
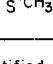
^a Assumed to be absent when isobutane was absent.

^b Butadiene was present.

^c Value possibly high.

^d Gas phase equilibrium attained.

TABLE 6. PRODUCT DISTRIBUTION IN HYDRODESULFURIZATION OF SUBSTITUTED BENZOTHIOPHENE CATALYZED BY COBALT MOLYBDATE AT 673°K (GIVENS AND VENUTO, 1970)

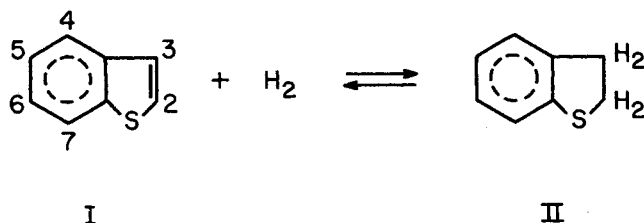
Reactant → Product, approximate mole %				
	R=H R=CH ₃	R=H R=CH ₃	R=H R=CH ₃	R=H R=CH ₃
	- 2	0.5 2	5 2	4 1
	- 4	0.5 0.5	0.5 -	- -
	96 86	6 7	10 10	3 1
	- -	5 3	42 22	2 2
	- -	75 54	18 10	8 4
Unidentified non-Sulfur Compounds	- 0.5	1 4	1 0.5	5 10
	Charge	1 8	2 11	- 2
	- -	Charge	18 26	15 14
	- -	9 14	Charge	15 17
	- -	- -	- -	Charge
Unidentified Sulfur Compounds	- 7	2 9	3 19	12 32

Data represent uncorrected peak areas by gas chromatography. Catalyst pretreated in hydrogen for 10,800 sec. at 823°K. Feed ratio hydrogen/benzothiophene was 3 to 5. Pressure assumed to be atmospheric.

reaction of thiophene and hydrogenation of butene but that it had very little effect on *cis-trans* isomerization, double bond shifts, and butadiene conversion to butenes. These results led to the suggestion that more than one kind of site is operative in hydrodesulfurization; we shall return to this suggestion.

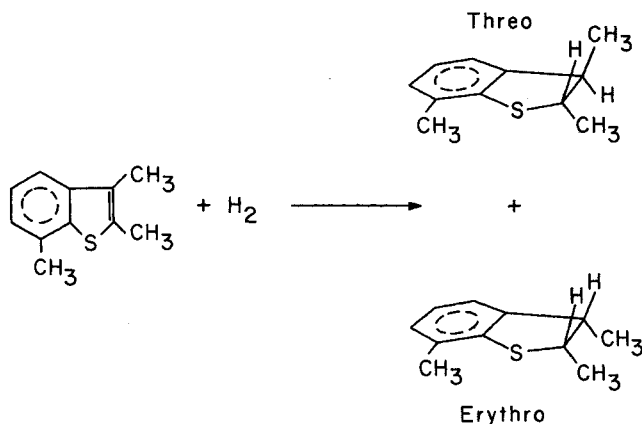
A study of the reaction network involved in hydrodesulfurization of substituted benzothiophenes was reported by Givens and Venuto (1970). Conversion data were obtained with a steady state flow reactor packed with particles of a commercial cobalt molybdate catalyst containing 2.4% Co and 6.7% Mo. Product distribution data for several feeds are collected in Table 6. Both desulfurized and undesulfurized products were found; some unidentified products were also found.

Givens and Venuto observed that a hydrogenation-dehydrogenation equilibrium was established at a rate which was high compared to the rate of desulfurization:



These two compounds were desulfurized at approximately equal rates, so it was impossible to establish whether one was an intermediate in the desulfurization of the other.

This information and the result that the hydrogenated compound (II) (dihydrobenzo[b]thiophene) was found as a product of reaction of the benzothiophene (I) at low temperature (573°K) and high space velocity (1.1×10^{-3} V/V/sec.) are consistent with identification of the hydrogenated compound as an intermediate in hydrodesulfurization of compound I. A similar set of results was obtained when the reactant was 2,3,7-trimethylbenzo[b]thiophene; two products identified as *erythro*- and *threo*-2,3-dihydro-2,3,7-trimethylbenzo[b]thiophene were found:



With some generality we may state that hydrogenated benzothiophenes (substituted and unsubstituted) are formed rapidly from benzothiophenes and hence that the former may be intermediates in the desulfurization although they cannot be unequivocally identified as such. These statements contrast with Amberg's results, which show that the hydrogenated compounds are not intermediates in hydrodesulfurization of the more reactive thiophene.

Possible pathways for desulfurization of the hydrogenated compound 1-methyldihydrobenzo[b]thiophene are shown in Figure 3. Neither of the mercaptan intermediates

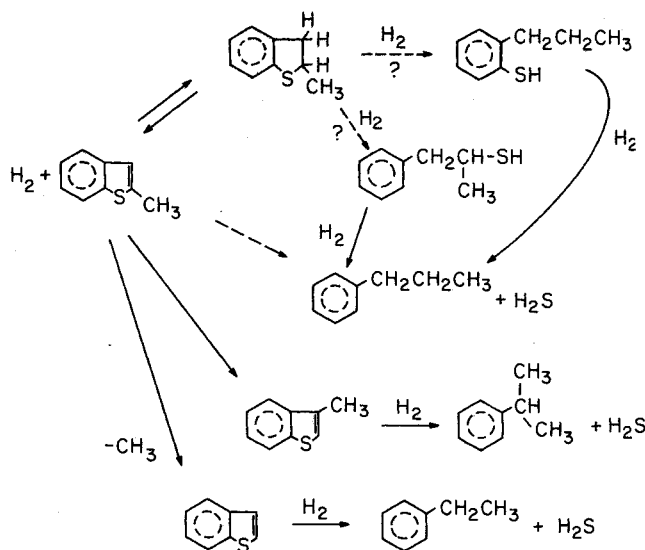


Fig. 3. Reaction network in hydrodesulfurization of benzothiophenes catalyzed by cobalt molybdate (Givens and Venuto, 1970).

TABLE 7. CONVERSION AND SELECTIVITY IN DESULFURIZATION OF SUBSTITUTED BENZO[b]THIOPHENES (GIVENS AND VENUTO, 1970)

Position of reactant methyl group(s)	None	7	2	2,7	3	3,7	2,3	2,3,7
Fraction of reactant converted	0.91-0.99	0.60	0.74	0.54	0.43	0.47	0.39	0.47
Fraction of reactant desulfurized	0.91-0.99	0.57	0.66	0.43	0.32	0.24	0.15	0.16
Selectivity, fraction desulfurized/fraction converted	1.00	0.95	0.89	0.80	0.75	0.51	0.38	0.34

Reaction conditions assumed to be those specified in Table 6.

TABLE 8. THIOPHENE HYDRODESULFURIZATION KINETICS: PARAMETER VALUES FOR EQUATIONS (1) AND (2) (SATTERFIELD AND ROBERTS, 1968)

Temp., °K	$10^9 \times k$, moles/ (kg sec N/m ²)	$10^4 \times$ K_T , m ² /N	$10^4 \times$ K_{H_2S} , m ² /N	$10^{10} \times k'$, moles/ (kg sec N/m ²)	$10^3 \times$ K'_B , m ² /N	$10^4 \times$ K'_{H_2S} , m ² /N
508	3.5	4.2	3.1	3.0	9.7	9.0
524	6.6	2.3	1.3	12.0	1.2	1.9
538	6.9	2.5	0.55	—	~0.0	1.3

TABLE 9. RANGES OF VARIABLES STUDIED IN HYDRODESULFURIZATION OF CYCLE OIL (FRYE AND MOSBY, 1967)

Temp., °K	533-643
$10^{-5} \times$ partial pressure of hydrogen, N/m ²	6.9-39
Hydrogen feed rate, std. m ³ /m ³ oil	89-356
$10^4 \times$ space velocity, kg oil/kg catalyst/sec	4.2-28
Sulfur content of oil, wt %	0.4-2.0

was detected, but neither pathway can be excluded since at these conditions mercaptans react about 10 to 100 times faster than the benzothiophene from which they might be formed.

Givens and Venuto were able to rule out desulfurization reactions involving C—C bond breaking by showing that the corresponding products were not formed. Saturation of the aromatic ring was found not to be necessary before breaking of the bond between sulfur and aromatic carbon could occur.

Using the appropriate intermediates shown in Figure 3 as feeds, Givens and Venuto demonstrated that primary sulfur extrusion, alkyl migration on the thiophene ring, and dealkylation of the thiophene ring all occur during hydrodesulfurization of 2-methylbenzo[b]thiophene at 673°K and atmospheric pressure.

The data of Table 6 for related feeds are consistent with this network; they show further that neither dealkylation nor migration of methyl substituents on the benzene ring of benzo[b]thiophene occurs appreciably at the reaction conditions.

The additional data of Table 7 lead to further general conclusions:

1. An increase in the number of substituent methyl groups leads to decreased reactivity of the benzothiophene and to a decreased selectivity for hydrodesulfurization.

2. The reactivity is significantly lowered by the presence of methyl substituents on the thiophene ring, especially in the 3-position; a methyl group on the benzene ring in the 7-position reduces the reactivity less.

In summary we can draw the following conclusions about the reaction networks in hydrodesulfurization:

1. Hydrodesulfurization of thiophene proceeds through butadiene and not through a hydrogenated compound. However, as the reactivity of the thiophene ring is decreased by addition of a benzene ring (giving benzothiophene), the rate of hydrodesulfurization becomes low

compared to the rate of hydrogenation of the thiophene ring, and the hydrogenated compounds may be intermediates.

2. The reactivities of compounds in the class of substituted benzothiophenes vary significantly, indicating there is little possibility of concisely summarizing results in terms of the reactivities of a small number of compound classes.

There is need for extending these investigations to include other reactants, especially less reactive ones, to obtain similar data for other catalysts, especially nickel molybdates, and to study the reactions at high pressures in the presence industrial feed and product components. A particularly interesting question concerns the role of intermediate olefins in coke formation and the rates of formation of olefin and coke as a function of catalyst composition.

Kinetics. There is a lack of thorough studies of hydrodesulfurization kinetics including effects of all reactants and products. A useful, though incomplete, determination of kinetics of thiophene hydrodesulfurization in the absence of mass transfer influence was reported by Satterfield and Roberts (1968), who used a commercial cobalt molybdate catalyst containing about 3% Co and 7% Mo. Reaction rate data were determined from low conversions attained in a steady state recirculation flow reactor. Pressure was slightly in excess of atmospheric, temperature was 508 to 538°K, and feeds contained various concentrations of thiophene and H₂S; hydrogen partial pressure was varied only insignificantly.

The products observed by Satterfield and Roberts are consistent with Amberg's reaction network (Figure 2). The data for rates of thiophene disappearance (hydrogenolysis) and rates of butane formation (butene hydrogenation) were correlated with Langmuir-Hinshelwood rate equations as follows:

$$r_{HDS} = \frac{k K_T P_T P_{H_2}}{(1 + K_T P_T + K_{H_2S} P_{H_2S})^2} \quad (1)$$

$$r_{Hyd} = \frac{k' K_B' P_B P_{H_2}}{(1 + K_B' P_B + K'_{H_2S} P_{H_2S})} \quad (2)$$

Values of the rate equation parameters are summarized in Table 8. Although the appropriateness of these equations is not firmly established (the dependence on hydrogen partial pressure, for example, was assumed), there are qualitative results which are clear: (1) H₂S inhibited

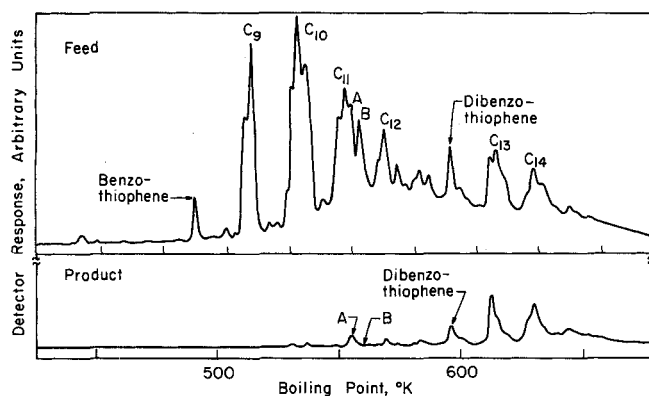


Fig. 4. Gas chromatographic analysis of benzothiophenes in desulfurized and undersulfurized cycle oil. Reaction at 603°K and 2×10^6 N/m² (Frye and Mosby, 1967).

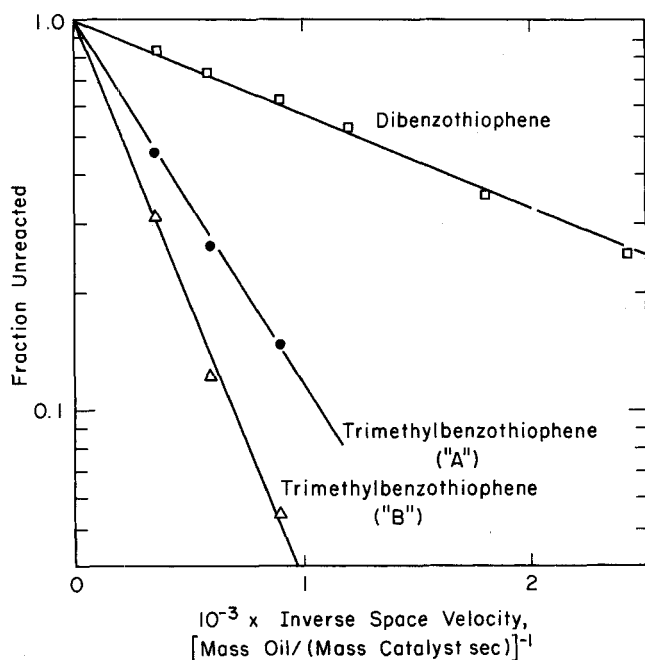


Fig. 5. Pseudo first-order hydrodesulfurization of benzothiophenes in cycle oil at 563°K and 1.5×10^6 N/m² (Frye and Mosby, 1967).

both the hydrogenolysis and hydrogenation reactions; (2) Significant amounts of reactant thiophene and butene were adsorbed on the catalyst surface in competition with H₂S. Less clear, but more important, is the conclusion that the hydrogenolysis and hydrogenation reactions proceed on separate catalytic sites, consistent with earlier results of Amberg.

A kinetic study of hydrodesulfurization of components in light catalytic cycle oils (boiling range about 450 to 600°K) was reported by Frye and Mosby (1967). Their reactor was a trickle bed containing particles of commercial cobalt molybdate catalyst of unspecified composition. The ranges of variables studied are given in Table 9. Feed and product analysis by gas chromatography provided data for evaluation of kinetics for individual sulfur compounds in the oil. Figure 4 includes chromatograms for feed and product; the results illustrate a general conclusion: low-molecular-weight compounds are more readily desulfurized than high-molecular-weight compounds. Detailed data for three components, a trimethylbenzothiophene (A), another trimethylbenzothiophene (B), and dibenzothiophene, are shown in Figure 5. For each sulfur-

containing compound, the fraction remaining unconverted decreased in proportion to the inverse space velocity. These results demonstrate that the hydrodesulfurization reactions are first order in the concentration of the sulfur compound. The difference in rate of desulfurization of isomers A and B is consistent with the cited results of Givens and Venuto.

Frye and Mosby stated that hydrodesulfurization was inhibited by H₂S and by aromatic hydrocarbons (presumably including those undergoing hydrodesulfurization), which is consistent with Satterfield and Roberts' Equation (1) and the results of other workers. The data of Figure 5 were presumably not corrected for changes in concentrations of these inhibitors accompanying depletion of the sulfur compounds.

Frye and Mosby also found that hydrodesulfurization was first order in hydrogen partial pressure for values less than 2.8×10^6 N/m², confirming the assumption incorporated in Equation (1).

Phillipson (1971) reported kinetics of desulfurization of thiophene and other sulfur compounds found in light distillates. The catalyst was cobalt molybdate containing 2% Co and 8% Mo. Vapor feeds contained heptane mixed with dimethyl sulfide, phenyl mercaptan, diethyl sulfide, tetrahydrothiophene, or thiophene. Steady state conversions were found to be independent of linear velocity through the catalyst bed, demonstrating the absence of significant interparticle mass transfer resistance. The absence of an effect of catalyst particle size at atmospheric pressure indicated the absence of significant intraparticle mass transfer resistance.

The hydrogenolysis of each sulfur compound was first order in the partial pressure of the sulfur compound, consistent with previously mentioned results. Reaction order was roughly 0.5 in hydrogen partial pressure and roughly -0.5 in heptane partial pressure, indicating that heptane was adsorbed competitively on catalytic sites. Rate increased in proportion to the square root of total pressure;

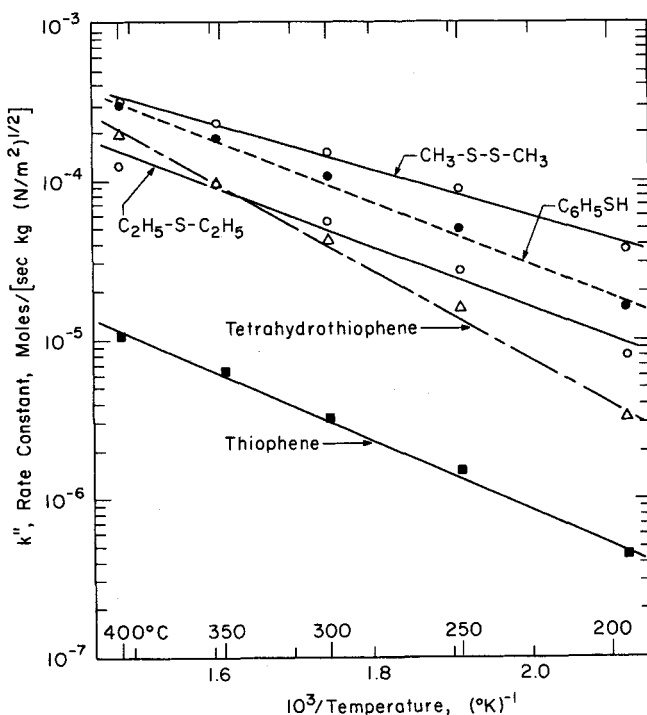


Fig. 6. Arrhenius plot for hydrodesulfurization of compounds in light petroleum distillates. Rate constant k'' defined by Equation (3) (Phillipson, 1971).

the author ascribed this result to intraparticle mass transfer influence at pressures exceeding atmospheric, but catalyst particle size was not varied to test the hypothesis. Reaction was inhibited by H_2S . The empirical rate equation is of the following form:

$$r = \frac{k'' P_S P_{H_2}^{1/2} P_{total}^{1/2}}{P_{HC} (1 + K'' H_2S P_{H_2S})} \quad (3)$$

The experimental values of the rate constant are shown in Figure 6. They demonstrate the lack of reactivity of thiophene compared to mercaptans, sulfides, and disulfides. These data are reported to be useful in design of light distillate desulfurization reactors, but they are of little use for heavier distillates such as kerosene and gas oils, which contain significant amounts of less reactive compounds such as benzothiophene (Phillipson, 1971). Experiments are needed to determine kinetics of hydrodesulfurization of these less reactive compounds at industrial reaction conditions.

The inhibiting effect of H_2S has been determined by Metcalfe (1969) for distillate hydrodesulfurization catalyzed by cobalt molybdate:

$$k_{effective} = k \frac{1}{1 + 21(P_{H_2S}/P_{total})} \quad (4)$$

In this equation k is a pseudo first-order rate constant, and $k_{effective}$ is a corrected value incorporating the effect of H_2S inhibition. When the H_2S level becomes 0.3 mole % in the reactant gas mixture, the reaction rate is reduced by about 5%; these values may be representative of complete reaction of nonthiophenic sulfur compounds in light distillates (Phillipson, 1971).

Cecil et al. (1968) represented H_2S inhibition by the same form of equation. For hydrodesulfurization of an unidentified gas oil with an unidentified catalyst, the reaction rate was reduced about twofold when 10 mole % of the treat gas was H_2S . Correspondingly, the rate would be reduced by about 5% when the gas contained 0.5% H_2S , which indicates that the results are similar to Metcalfe's for light distillates.

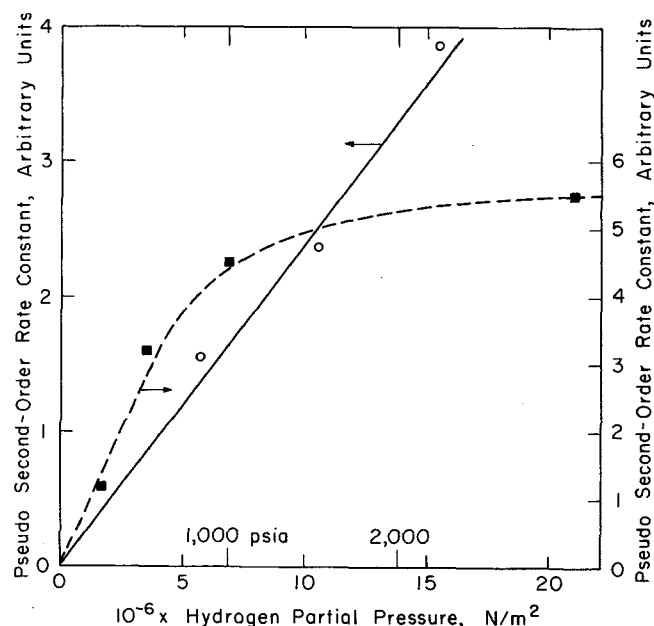


Fig. 7. Dependence of hydrodesulfurization rate on hydrogen partial pressure. Solid line for unidentified Middle Eastern residuum (Cecil et al., 1968); dashed line for Kuwait atmospheric residuum (Beuther and Schmid, 1963).

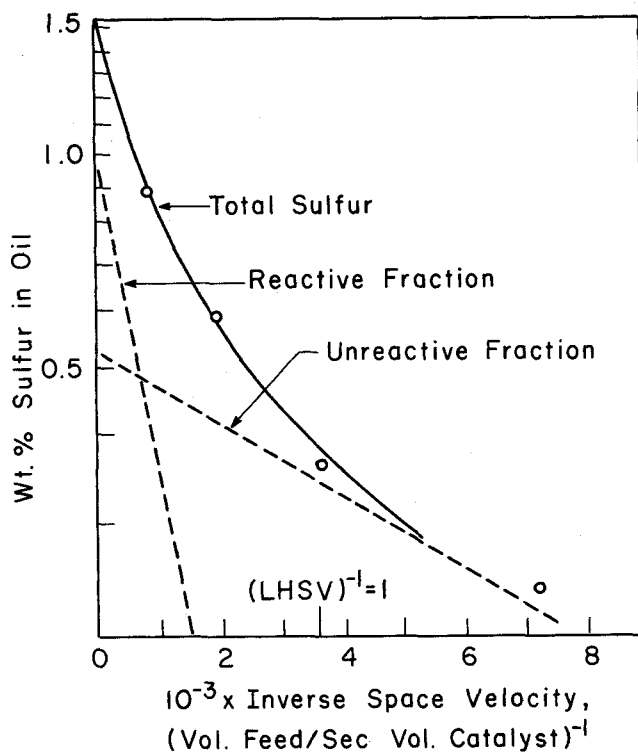


Fig. 8. Hydrodesulfurization of Venezuelan vacuum gas oil: Two-component, pseudo first-order kinetics (Cecil et al., 1968).

Simplified Kinetics for Industrial Feedstocks. Many of the kinetic results cited for pure compounds are observed generally for hydrodesulfurization of distillates and residua. Reaction is inhibited by product H_2S and is first order in hydrogen partial pressure at sufficiently low values. The data of Cecil et al. (1968) (Figure 7), for example, demonstrate that with an unidentified catalyst, rate of desulfurization of a Middle Eastern residuum is proportional to hydrogen partial pressure over a range of 0.14×10^7 N/m². However, Beuther and Schmid (1963), for example, observed that beyond 7×10^6 N/m² there was only a small effect of increased hydrogen partial pressure on rate of residuum hydrodesulfurization (Figure 7). The sparse and conflicting results suggest a dependence of the kinetics on catalyst composition and on the nature of the feedstock. The catalyst surface may become saturated with hydrogen at pressures of the order of 7×10^6 N/m², and the saturation pressure may depend on the surface structure and the amounts of competitively adsorbing hydrocarbon species.

The rate of hydrodesulfurization of any feed is generally consistent with the first order reaction of each of a series of sulfur-containing compounds, as is to be expected from the foregoing discussion. The results of Cecil et al. (Figure 8) show a typical curve for total sulfur concentration as a function of inverse space velocity. The shape of the curve is very close to that expected for a second order dependence of rate on total feed sulfur content—this generally observed result is useful for process design.

A more firmly based analysis involves considering the feed as a mixture of sulfur-containing compounds, each of which reacts at a rate proportional to its concentration. Often the curve for total sulfur content versus inverse space velocity is approximated as if there were only two reactive components. The two straight lines in Figure 8 indicate first order reaction of each of the hypothetical two components; these lines sum to a curve representing the data. We may write the following rate equation, which is useful for design:

TABLE 10. DISTRIBUTION OF THIOPHENIC SULFUR IN MIDDLE EASTERN GAS OIL (CECIL ET AL., 1968)

	wt % of Thiophenic Sulfur in the Fraction				
Boiling range, °K	644-672	672-700	700-727	727-755	755-782
Thiophenes	2.4	2.2	2.2	2.6	1.8
Benzothiophenes	31.5	26.5	27.5	28.9	32.2
Dibenzothiophenes	50.8	50.8	47.6	38.5	36.5
Benzonaphthothiophenes	15.3	20.5	22.7	30.0	29.5

$$r_{\text{HDS}} = \alpha_1 k_1 c_S + \alpha_2 k_2 c_S \quad (5)$$

The integrated form for a piston-flow reactor is then

$$\frac{c_S}{c_{S0}} = \alpha_1 e^{-k_1/LHSV} + \alpha_2 e^{-k_2/LHSV} \quad (6)$$

This simplified representation of the kinetics is valid only when partial pressures of hydrogen and H_2S are held constant; these values are incorporated in k_1 and k_2 .

As van Deemter (1965) has pointed out, for many practical reactor designs the reactive fraction will be almost completely removed from the product, and the design can be based on the other fraction (referred to as the unreactive fraction) alone. This simplification reduces the intrinsically complex kinetics to first order. The unreactive fraction is not to be confused with a single sulfur-containing compound. The adjustable parameters α_2 and k_2 are to be determined empirically for each feed and catalyst.

It is to be expected that α_2 , the fraction of the sulfur compounds which are unreactive, will increase with increasing feed boiling range; correspondingly k_2 , the rate constant for the unreactive fraction, is expected to decrease with increasing feed boiling range. Cecil et al. (1968) have presented data (Table 10) which show the concentration of components in the thiophenic sulfur fraction in the high boiling fractions of a Middle Eastern gas oil. The very unreactive benzonaphthothiophenes are concentrated in the highest boiling fractions.

For petroleum feedstocks we may summarize the intrinsic kinetics in the following equation, which accounts

approximately for all the cited effects:

$$r_{\text{HDS}} = \frac{\alpha_2 k_2 p_{\text{H}_2} c_S}{(1 + K_{\text{H}_2} p_{\text{H}_2} + K_{\text{H}_2\text{S}} p_{\text{H}_2\text{S}})} \quad (7)$$

The equation is written for the unreactive fraction of sulfur only, hence it is useful only for high conversions.

Inhibition of reaction by H_2S is accounted for by the denominator term; the reaction is first order in hydrogen partial pressure at low values and zero order at high values. Competitive adsorption of unreactive petroleum compounds is not explicitly accounted for; terms of the form $K_i c_i$ in the denominator might be appropriate additions.

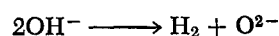
It is clear that an equation of the form of Equation (7) is not sufficient for process design calculations. Account must also be taken of mass transfer effects and of catalyst aging, which affects both the mass transfer and the intrinsic kinetics. These effects are to be considered subsequently.

Catalysts

The Alumina Support. Hydrodesulfurization catalysts most often contain alumina as a support, typically having a surface area of the order of 2 to $3 \times 10^5 \text{ m}^2/\text{kg}$, a pore volume of about $5 \times 10^{-4} \text{ m}^3/\text{kg}$, and an average pore diameter of about 10 nm . Of the various types of alumina available, $\gamma\text{-Al}_2\text{O}_3$ appears to be the one generally applied. Since the chemical nature of this support may be important to the surface chemistry of hydrodesulfurization, a discussion of the properties of alumina is presented here (see Newsome et al., 1960; van Reijen, 1964; and Lippens, 1961).

The aluminas are invariably prepared by precipitation of a hydrated alumina formed by mixing solutions of alkali and salts of an aluminum compound (sulfate, nitrate, or occasionally chloride). The precipitate formed is gelatinous with a diffuse x-ray diagram resembling that of the mineral boehmite, $\text{AlO}(\text{OH})$, (gelatinous boehmite). The precipitate is usually aged by gentle heating in an aqueous slurry, the aging conditions determining the properties of the final product. Aging at 313°K produces a solid which has an x-ray diagram more closely akin to that of bayerite $\text{Al}(\text{OH})_3$. If subsequently aged at 353°K , the solid is converted into a product, again similar in its x-ray diagram to boehmite, which is now in a much more highly crystalline form (crystalline boehmite). Alternatively, aging in an alkaline solution leads to a different form of $\text{Al}(\text{OH})_3$, gibbsite, which usually contains some alkali.

Subsequent to the wet stages in the synthesis, the precipitate is filtered and calcined at a temperature of about 875°K . The calcination leads to elimination of water, either that initially present as such in the wet precipitate, or that formed by reaction of $-\text{OH}^-$ groups in a more advanced stage of the calcination:



As this latter process of water elimination takes place,

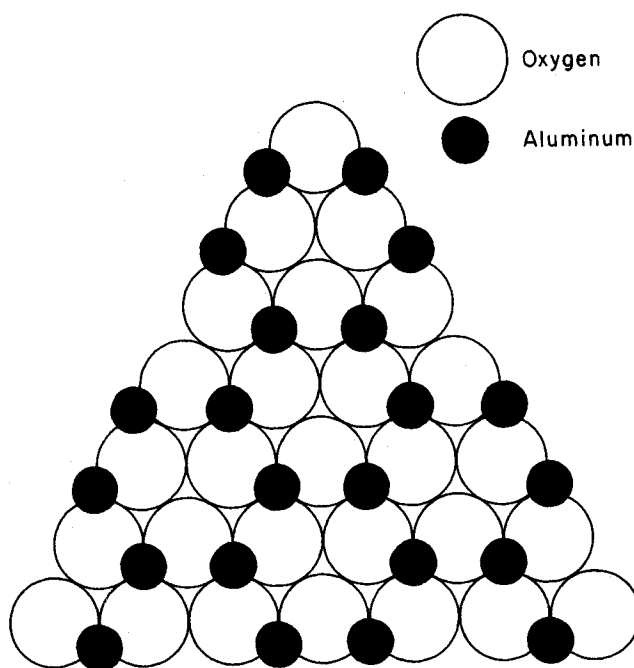


Fig. 9. Arrangement of Al^{3+} ions in $\alpha\text{-Al}_2\text{O}_3$.

the surface area starts to increase as pores are formed; the surface area later decreases as sintering occurs. At calcining temperatures higher than 1610°K the product is invariably α - Al_2O_3 , having low surface area and no longer containing either water or $-\text{OH}^-$ groups. The structure of α - Al_2O_3 is a hexagonal close packing of O^{2-} ions with Al^{3+} ions in the octahedral interstices between the oxygens. Since there are as many octahedral interstices (sites) as O^{2-} ions, stoichiometry indicates that one in every three sites remains empty. The distribution of Al^{3+} ions among the available sites in α - Al_2O_3 is illustrated in Figure 9, which shows a close packed layer of O^{2-} ions with the Al^{3+} ions positioned on top of this layer. The next layer of O^{2-} ions is situated in positions 2 (Figure 10), the stacking sequence being 1-2-1-2-...

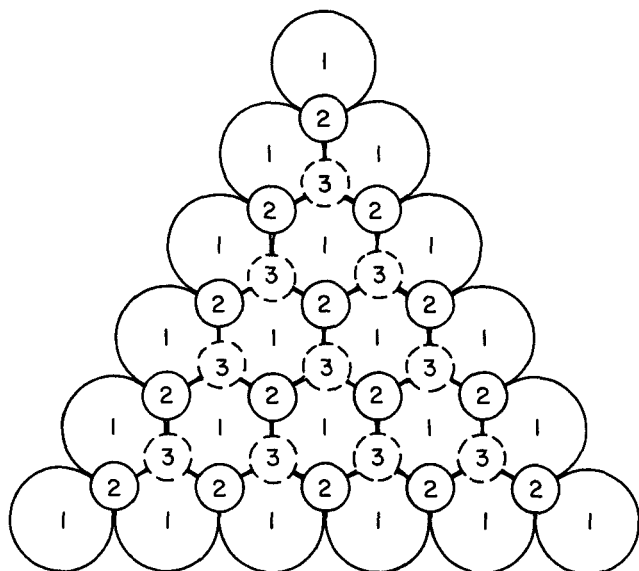


Fig. 10. Close packing structures: Hexagonal, sequence 1-2-1-2-...; Cubic, sequence 1-2-3-1-2-3-...

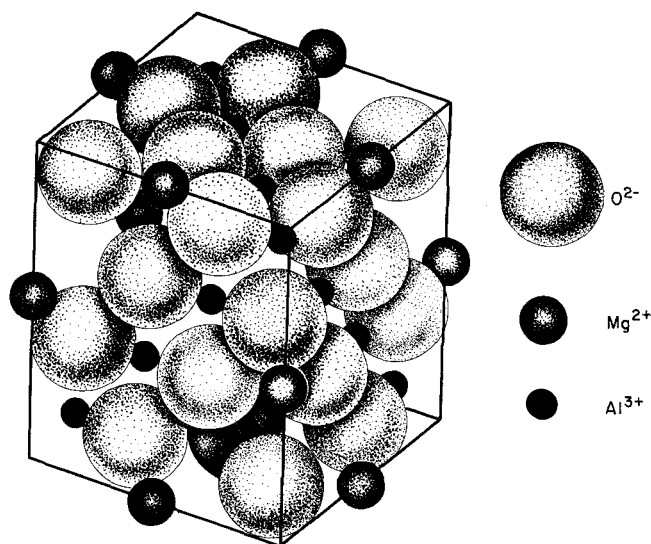


Fig. 12. Unit cell of spinel (MgAl_2O_4) (Kittel, 1971).

TABLE 11. PREPARATION OF ALUMINAS

	hydrated alumina	gelatinous boehmite	bayerite	crystalline boehmite	gibbsite
Calcination temperature, °K					
875			η - Al_2O_3	γ - Al_2O_3	χ - Al_2O_3
1175			θ - Al_2O_3	δ - Al_2O_3	κ - Al_2O_3
>1375			α - Al_2O_3	α - Al_2O_3	α - Al_2O_3

Since calcination initially involves the trihydrates $\text{Al}(\text{OH})_3$, their structures are also considered here. Both bayerite and gibbsite are layer structures in which two layers consisting of close-packed OH^- ions surround the Al^{3+} ions. The Al^{3+} ion arrangement in the hydroxide is different from that in α - Al_2O_3 (see Figure 11) and consists of rows of parallel interstices, two of three being occupied (van Reijen, 1964). During the calcination, a number of intermediate structures are observed; since a catalyst support usually consists of one of these, they are of importance here, particularly the η -, γ -, and, to a lesser degree, the χ -aluminas (Table 11).

These still contain water, presumably entirely as $-\text{OH}^-$ groups at surfaces, the overall composition being $\text{Al}_2\text{O}_3 \cdot n\text{H}_2\text{O}$, with $0 < n < 0.6$. In both η - and γ - Al_2O_3 the oxygen ions are cubic close packed. This packing is characterized by a slightly different type of stacking of the close packed oxygen layers (Figure 10), that is, 1-2-3-1-2-3-... Further, there is a change in the Al^{3+} ion distribution; instead of being confined to the octahedral interstices, some of the cations are now in tetrahedral sites, hence they are tetrahedrally surrounded by O^{2-} ions. In a cubic close packing of anions there are one octahedral and two tetrahedral sites per anion. In spinels like MgAl_2O_4 the Al^{3+} ions occur in octahedral sites and the Mg^{2+} ions in tetrahedral sites. (See Figure 12 for the unit cell of MgAl_2O_4 , which has 32 O^{2-} ions; 32 octahedral sites [half occupied by Al^{3+} ions]; and 64 tetrahedral sites [8 occupied by Mg^{2+} ions]). Because of the similarity in structure of the aluminas and the spinels, the former are often referred to as pseudo-spinels. Introducing a notation in which tetrahedral and octahedral Al are given

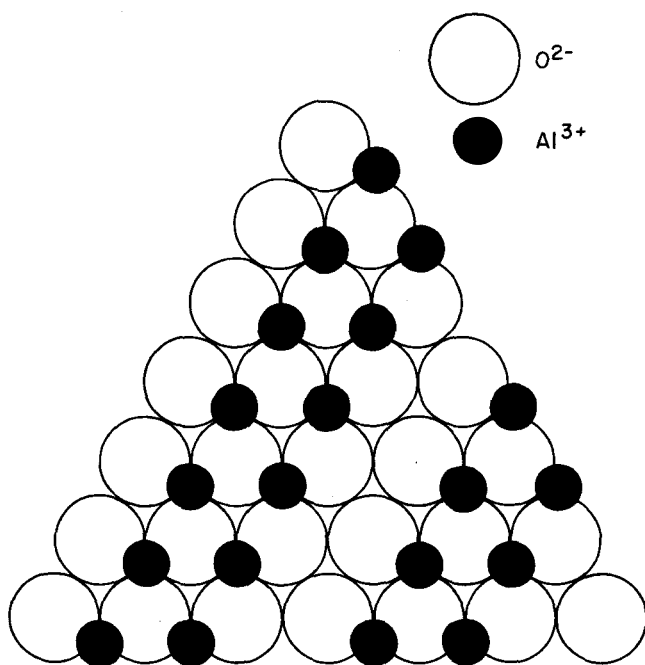


Fig. 11. Arrangement of Al^{3+} ions in $\text{Al}(\text{OH})_3$.

as $[Al]_t$ and $[Al]_o$, we represent the aluminas as $[Al_{2/3}]_t [Al_2]_o O_4$.

The differences between η - and γ - Al_2O_3 are probably related to their different ratios of $[Al]_t:[Al]_o$ as well as to the different distributions of $[Al]_t$ over the available tetrahedral sites and $[Al]_o$ over the octahedral sites. Lippens (1961) proposed the models for η - and γ - Al_2O_3 shown in Figures 13a and b.

In discussing Lippens' η - Al_2O_3 structure we start again from the close packed oxygen layer of Figure 9 (the (111) plane in the cubic close packing). There are now two types of arrangements of the Al^{3+} ions. One (the B-layer) is the same as that of Figure 9, while the other (the A-layer) is derived from this by transferring two-thirds of the cations from octahedral to tetrahedral sites. The stacking of the layers is A-B-A-B-...

The γ - Al_2O_3 structure is more easily visualized starting from the (110) crystal plane which is oriented at a certain angle with respect to the (111) plane. Again there are two types of layers, the C- and D-layers. The D-layer has only octahedral cations, and the C-layer has as many tetrahedral as octahedral sites. The packing sequence is C-D-C-D-...

An important subject for the present discussion is the type of surface which is to be expected from the structure of the solid. The aluminas occur in the form of lamellae,

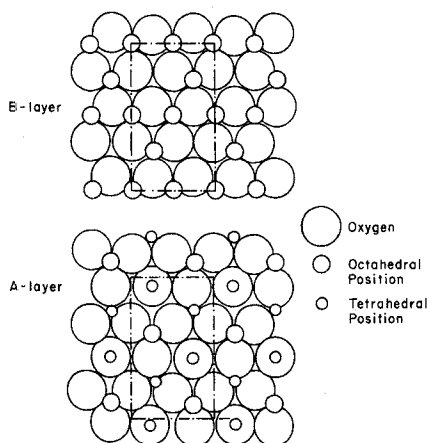


Fig. 13a. Structure in η - Al_2O_3 (Lippens, 1961).

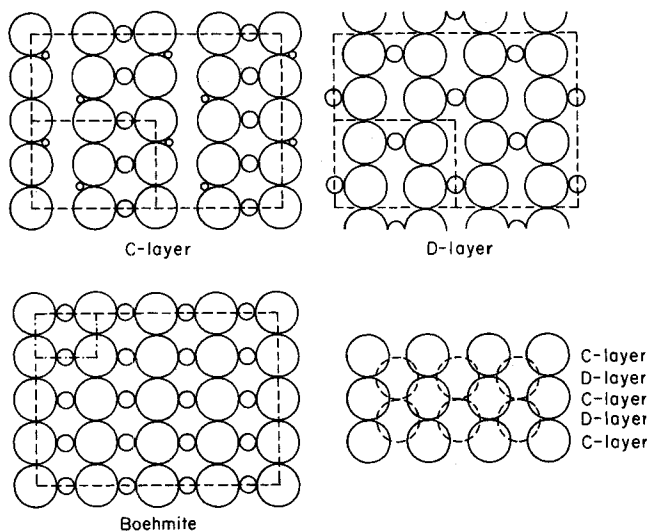


Fig. 13b. Structure in γ - Al_2O_3 (Lippens, 1961).

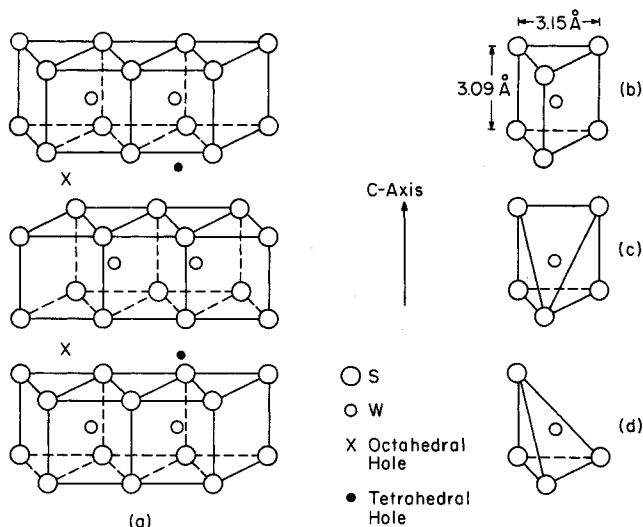
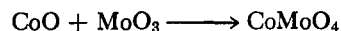


Fig. 14. Structure of WS_2 : (a) stacking of layers illustrating the position of octahedral holes which may be partly occupied by Ni; (b) site symmetry of W^{3+} ions in the bulk; (c) in the sideface; and (d) in an edge parallel to the c-axis (Voorhoeve and Stuiver, 1971 b).

so it may be expected that one type of surface plane is predominant. According to Lippens this is the (111) plane for η - Al_2O_3 and the (110) plane for γ - Al_2O_3 .

Interaction of Promoter and Catalyst. During preparation when the potential catalyst is still in the oxide state, interactions may occur between compounds such as MoO_3 or WO_3 (the catalyst precursors), on the one hand, and CoO or NiO (the promoters), on the other. For instance,



Later in the catalyst preparation when reduction and sulfiding occur, these binary oxides might be converted into binary sulfides, and their identification in an early stage of the catalyst preparation is therefore important.

There has been extensive research into the class of compounds represented by the formula ABO_4 , where A is a divalent transition metal ion (such as Co^{2+}) and B a hexavalent ion (such as Mo^{6+}). The structures are now fairly well understood owing to the work of Smith and Ibers (1965) and Sleight and Chamberland (1968). In all cases the coordination of the divalent cation is essentially octahedral, although the octahedra are distorted. The materials are dimorphic and sometimes even trimorphic, and the essential differences among the forms are in the coordination of the hexavalent cations; this coordination is either octahedral or tetrahedral.

There is no indication of these binary oxides in the x-ray diagrams of industrial catalysts, though this is hardly a proof of their absence. Magnetic susceptibility data are more informative. The paramagnetic species are the promoter cations Co^{2+} and Ni^{2+} ; their paramagnetism is dependent on the type of coordination because quenching of the orbital magnetic moment differs for the octahedral and tetrahedral coordinations, being more complete for the latter. Griffith (1961) calculated the magnetic susceptibility of Co^{2+} to be 4.68β (Bohr magnetons) in octahedral and 3.87 in tetrahedral surroundings, and Cossee (1956) gave experimental values of 4.7 to 5.1 and 4.0 to 4.1β respectively.

Lipsch (1969; Lipsch and Schuit, 1969a, b, c) measured the paramagnetic susceptibilities of the two forms of $CoMoO_4$ and found values of 5.4 and 4.7β , in good agreement with the prediction. Lipsch also investigated a commercial hydrosulfurization catalyst (Ketjenfine)

and found its paramagnetic susceptibility to be 4.2β . He concluded that there is no CoMoO_4 in this catalyst; what is actually present will be discussed later. Richardson (1964), who preceded Lipsch in applying magnetic measurements to commercial hydrodesulfurization catalysts, reported that most of the Co^{2+} was present as CoAl_2O_4 but that a small fraction might be present as CoMoO_4 ; this was inferred to have abnormal properties since, unlike bulk CoMoO_4 , it was resistant to treatment by H_2 and H_2S . This CoMoO_4 was considered by Richardson to be responsible for the catalytic activity.

The reduction of MoO_3 or WO_3 by hydrogen in the presence of sulfur-containing compounds is usually considered to give rise to MoS_2 or WS_2 . These compounds have a layer structure, discussed in detail by Voorhoeve (1971), Voorhoeve and Stuiver (1971 a, b), and Farragher and Cossee (1972). Disulfides of Nb, Mo, Ta, and W all have layer structures in which the metal is surrounded by a trigonal prismatic coordination of six sulfur atoms (see Figure 14). The stacking of the sulfur layers is hexagonal or rhombic, and defect structures are common. In trigonal prismatic coordination the d-orbitals of the metal split into a lower A' (single) and two doubly degenerate groups, E' and E'' , which form bands (Huisman et al., 1971; Wilson and Yoffe, 1969). In NbS_2 and TaS_2 the band associated with A' is half-filled; in MoS_2 and WS_2 it is full.

The former two compounds, because of the ability to accommodate more electrons in the half-filled band, show the property of intercalation: in the empty sites between the double layers of sulfur, which contain Nb^{4+} and Ta^{4+} ions, metal atoms (such as Cu and Ag) can be accommodated which donate their electrons to the A' band. In an ideal crystal of MoS_2 or WS_2 , however, these electrons would have to be accommodated in the E' bands, which is unlikely because of the energetically less favorable positions of these bands. Intercalation therefore does not occur in MoS_2 or WS_2 .

One compound involving Mo has been found, however, in which intercalation can occur (van den Berg, 1968; Chevrel et al., 1968). The structure of the compound was given by Miss van den Berg; it has the composition CoMo_2S_4 and the nominal formula $\text{Co}^{2+}\text{Mo}^{3+}_2\text{S}^{2-}_4$. Again it is a layer structure with Co located between the MoS_2 layers, the Mo now being octahedrally coordinated. Since the crystal-field splitting in octahedral coordination leads to a triply degenerate, lower T_2 level and a doubly degenerate, higher E level, the lower level can accommodate more electrons than in the trigonal prismatic coordination.

Although intercalation is not possible for ideal MoS_2 and WS_2 crystals, Voorhoeve and Stuiver and Farragher and Cossee postulated that in actuality it can occur to a certain extent provided the crystals are small. Voorhoeve's arguments are derived mainly from ESR data and the assignment by Voorhoeve and Wolters (1970) of a resonance at 3,250 Oe to W^{3+} . The resonance was observed in sulfur-deficient $\text{WS}_{1.95}$ but not in stoichiometric WS_2 ; it increased with surface area and with the amount of Ni. For pure WS_2 the signal strength was of the order of 10^{14} to 10^{15} spins (Mo^{3+} ions) per m^2 , increasing by a factor of 10^2 on insertion of a small amount of Ni (0.016 Ni per W). For high contents of Ni the signal intensity was linearly dependent on the surface area. Voorhoeve therefore concluded that intercalation of Ni is to be ascribed to the existence of edges on the layers, and Farragher and Cossee estimated that because of the smallness of the MoS_2 or WS_2 crystals in commercial catalysts, the intercalation could increase to values of Co:Mo or Ni:W of about 0.3 to 1.0.

Although Farragher and Cossee considered their structural model to be applicable as well to Co and MoS_2 , the ESR data for these compounds do not appear to confirm its extension. Lo Jacono et al. (to be published) did not find signals other than that for Mo^{5+} after reducing $\text{MoO}_3/\gamma\text{-Al}_2\text{O}_3$ with $\text{H}_2 + \text{H}_2\text{S}$. In the compound CoMo_2S_4 a signal at $g = 2.17$ was found by Chevrel et al. (1968), and a similar signal has been observed by Lo Jacono et al. after treatment of $\text{CoO}/\text{MoO}_3/\text{Al}_2\text{O}_3$ catalysts by $\text{H}_2 + \text{H}_2\text{S}$ followed by H_2 . The signal, however, was also observed with a greater intensity in similarly treated $\text{CoO}/\gamma\text{-Al}_2\text{O}_3$; it is therefore almost certainly to be attributed to some form of cobalt.

An interesting observation related to the mechanism of the sulfiding process was made by Seshadri et al. (1970); they found that ESR spectra of sulfided $\text{CoO}/\text{MoO}_3/\gamma\text{-Al}_2\text{O}_3$ samples showed a triplet, which was assigned to polymeric sulfur radicals. The experiments were repeated by Lo Jacono et al. (1972), who found that the signal was not present in the pretreated samples but came into existence only when a sample was exposed to air after the pretreatment. A complete explanation of these observations must await further research.

Interaction of Catalyst Components with the Support. The relatively low paramagnetic susceptibility of Co-impregnated $\gamma\text{-Al}_2\text{O}_3$, first found by Richardson (1964), was attributed by him to the formation of the spinel CoAl_2O_4 . The presence of this compound was ascribed to an interaction of CoO and $\gamma\text{-Al}_2\text{O}_3$ in which the Co^{2+} occupied the tetrahedral interstices in the alumina lattice, confining the Al^{3+} to the octahedral sites. He considered this form of Co^{2+} to be unimportant to the catalytic activity. Ashley and Mitchell (1968 a, b), using both magnetic and spectroscopic (reflection) measurements in the visible-uv spectrum, also concluded that Co^{2+} was present in tetrahedral sites, but these authors did not agree that CoAl_2O_4 was formed. Lipsch, however, obtained data from similar measurements and did agree to the existence of CoAl_2O_4 .

Spectroscopic measurements are particularly suitable for identification of Co^{2+} (tetrahedral) because they refer to a local symmetry (point-group symmetry) associated with relatively intense spectral d-d transitions. (The blue color of $\text{CoO}/\text{MoO}_3/\text{Al}_2\text{O}_3$ catalysts is probably due to this species.) Because of the intensity of the Co^{2+} (tetrahedral) spectra, the simultaneous presence of Co^{2+} (octahedral), known to have spectroscopic transitions an order of magnitude weaker, becomes masked. Moreover, the spectra yield information concerning only the local symmetry; this symmetry might be similar to that in the spinel CoAl_2O_4 , even if the spinel were not actually formed. Lo Jacono et al. (to be published) therefore chose to describe the structure as a sub-surface spinel-like structure.

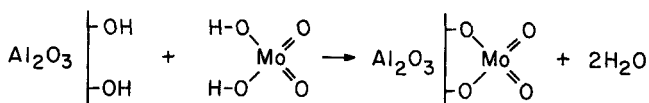
The ESR results of Lo Jacono et al. (to be published) led them to assign a special resonance at 1200 Oe to the tetrahedrally surrounded Co^{2+} and to conclude that it is indeed present within the $\gamma\text{-Al}_2\text{O}_3$ lattice. In accordance with results of earlier authors (Richardson, Lipsch), their spectra were not changed by treatment of the sample with $\text{H}_2 + \text{H}_2\text{S}$. They found no indication of Co^{2+} (octahedral), which is not too surprising because its signal could be broadened out of observation by spin-lattice relaxation. They did however find that relatively high concentrations of Co led to the formation of ferromagnetic materials (presumably mixtures of Co metal + CoS) after treatment with $\text{H}_2 + \text{H}_2\text{S}$. Tomlinson et al. (1961) and Keeling (1959) had previously concluded that a separate Co_3O_4 phase was present under similar conditions. Whatever it is, this phase is eliminated by the

presence of MoO₃.

The interaction of NiO with γ - and η -Al₂O₃ was investigated by Lo Jacono et al. (1971). As was to be expected from crystal-field considerations, the tendency of Ni²⁺ to occur in tetrahedral sites is appreciably less than that of Co²⁺; Ni²⁺ never occupies more than 25% of the total. The occurrence of tetrahedral Ni²⁺ is considerably greater in η - than in γ -Al₂O₃, and increased concentrations are favored by firing in dry rather than wet atmospheres.

The interaction of MoO₃ with the Al₂O₃ support has been discussed in differing interpretations by Ashley and Mitchell, Lipsch and Schuit, and Asmolv and Krylov (1970). Data were taken from IR spectroscopy and reflection spectroscopy in the visible-uv. Lipsch did not find much difference between unsupported and supported MoO₃, but there was an increased intensity and a stronger dispersion in the latter, which he concluded was evidence of an interaction of Mo⁶⁺ with the surface. Ashley and Mitchell believed the Mo⁶⁺ was predominantly tetrahedrally surrounded, which suggests a relatively strong interaction with the support, since in Al₂(MoO₄)₃ the Mo⁶⁺ is known to be tetrahedrally surrounded. Asmolv and Krylov also tended toward the assumption of tetrahedral Mo⁶⁺, especially at lower concentrations.

An ESR study of MoO₃ on η - and γ -Al₂O₃ was reported by Dufaux et al. (1970). If MoO₃ is calcined at temperatures around 750°K, it usually exhibits a weak signal at $g = 1.93$, which is assigned to Mo⁵⁺ in tetragonal square configuration. When η -Al₂O₃ was impregnated with ammonium molybdate, the resulting samples showed an intensity of this signal proportional to the MoO₃ content. The MoO₃ therefore appears to have been present as such. For γ -Al₂O₃, however, no Mo⁵⁺ signal was observed below 10 wt. % MoO₃, suggesting that the MoO₃ interacted with the support. The authors ascribed the result to the formation of the monolayer of MoO₃ on the surface of the support, as follows:



A similar model had been proposed earlier by Lipsch.

Lo Jacono et al. (to be published) found for MoO₃ contents exceeding the 10% limit that addition of increasing amounts of CoO led to a decrease in the Mo⁵⁺ signal. The observation might be attributed to the formation of CoMoO₄. Since, however, the intensity of the Co²⁺ (tetrahedral) signal did not decrease with the amount of MoO₃ present (it actually increased somewhat), this explanation is inadequate. Indeed the results even seem to indicate that Co increases the stability of the Mo monolayers.

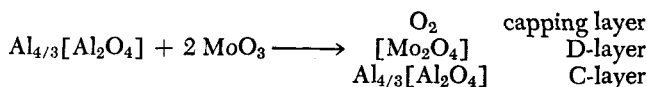
In the following paragraphs we present a new model for the monolayer structure.

The γ -Al₂O₃ is assumed to consist of particles formed by a one-dimensional stacking of C- and D-layers. The surface of a particle is assumed to consist entirely of these C- and D-layers, the ratio of the two types being one. The unit mesh of the surface planes is then either Al_{4/3}[Al₂O₄] or [Al₂O₄] for C- or D-layers, respectively. (The metal represented inside the brackets is octahedrally surrounded and that outside the brackets tetrahedrally surrounded.) A MoO₃ monolayer on the alumina surface is required to have a similar symmetry. If the outer layer of the support is a C-layer, the monolayer will have D-symmetry, and vice versa. Evidently such an arrangement would have an excess positive charge, and in compensa-

tion an anion layer is assumed to be located on top of the monolayer, with the maximum number of O ions per unit mesh being four.

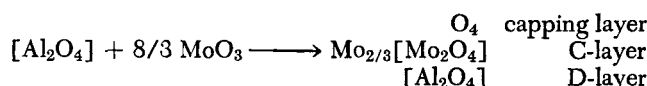
To facilitate further discussion, the outer alumina layer will be called the "surface layer;" the adjacent Mo layer, the "monolayer;" and the top layer consisting of only anions, the "capping layer."

If the surface layer is a C-layer (referred to as case Ia), the formation of the boundary layer can be written as



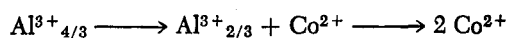
A monolayer with Mo as the cation is formed with D-symmetry, that is, with only two Mo cations per unit mesh, both in octahedral positions. The excess positive charge is compensated by a capping layer only half filled. All the oxygens in the monolayer are engaged in completing the surroundings of the Al ions in the surface layer. The monolayer is therefore firmly bonded to the surface.

For a surface D-layer (case IIa) one obtains

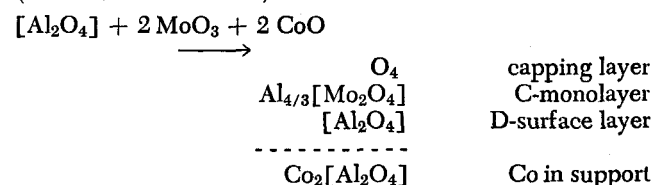


The monolayer should have C-symmetry and therefore contain both octahedral and tetrahedral Mo. The maximum number of Mo cations in this layer is however restricted by the capacity of the capping layer. With four O anions per unit mesh in the capping layer (that is, at full coverage), the monolayer content is restricted to 8/3 Mo ions. In the formula, the octahedral sites are fully occupied but the tetrahedral sites only partially; a different system of occupation with more tetrahedral and fewer octahedral Mo ions is evidently not excluded. Note that the full burden of binding the monolayer to the surface layer falls on the Mo component; if O ions are removed, for instance by reduction, the monolayer will have a tendency to become separated from the support. This arrangement is therefore considered less stable than the arrangement just given (case Ia).

Incorporation of Co²⁺ in the support, visualized for convenience as a reaction with CoO, is assumed to result in location of the cation in a tetrahedral position somewhere in a C-layer within the solid, hence below the boundary layer. Its accompanying O ion can find no position in the support and therefore remains at the surface, for example in the capping layer. Penetration of Co²⁺ ions into the support must be accompanied by expulsion of Al³⁺ ions from the support, since Co is replacing Al. The Al cations must find a position in the boundary layer. The replacement reaction is then as follows:



A simultaneous introduction of MoO₃ and CoO is readily visualized when the surface layer is a D-layer (referred to as case IIb):



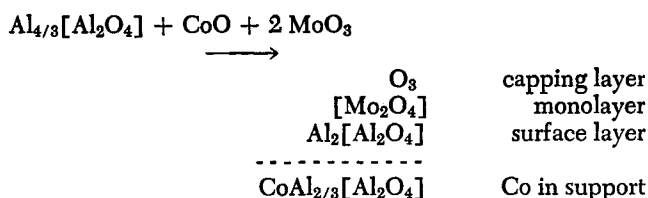
Two Co ions per unit mesh are incorporated within the solid, forcing 4/3 Al ions to the boundary layer where they occupy the tetrahedral sites in the monolayer. Fewer

Mo ions are therefore incorporated, and all of these must find positions in octahedral interstices. Since there is simultaneous incorporation of both Co and Mo, the capping layer remains complete, but the ratio [O (capping layer) : Mo (monolayer)] becomes greater than when Co was absent. The stability of the monolayer is increased because part of the task of binding the monolayer to the surface layer is taken over by Al.

When the surface layer is a C-layer, the simultaneous incorporation of MoO_3 and CoO is less readily understood. There are various possibilities:

Case Ib1: There is no place for the Al to be incorporated in the boundary layer, and hence there is no incorporation of Co via this part of the surface; the situation remains as for case Ia.

Case Ib2: The Al content in the surface layer can be increased somewhat because there are still tetrahedral sites available, but the ratio [Al (tetrahedral) : Al (octahedral)] becomes different from that in C-layers in the bulk:



Case Ib3: The Al ions become part of the capping layer. The monolayer is then covered by an inert layer and ceases to be catalytically active.

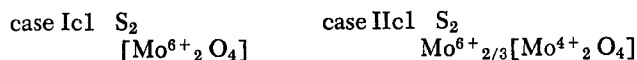
For the combination of cases Ib1 and I Ib, the maximum Co:Mo ratio would be 1/2; the combination including extra participation of incorporation via case Ib2 would give a ratio of 3/4 and that including participation via case Ib3 might even give a ratio of 1. Since in practical catalysts the Co:Mo ratio is often between 1/2 and 1,

cases Ib2 and Ib3 cannot be entirely excluded. Because of the inaccessibility of Mo in case Ib3, however, this possibility will be considered no further.

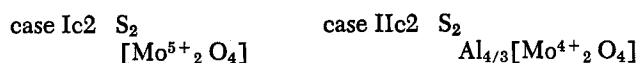
The actual catalyst operates in a reduced and (partially) sulfided state, that is, O^{2-} ions are removed from the boundary layer or exchanged by S^{2-} ions. It is now assumed that removal or exchange can occur in the capping layer only, since otherwise the connection between the surface layer and monolayer would be destroyed. Moreover, since S^{2-} is much larger than O^{2-} , the maximum number of S ions in the layer is fixed at two instead of four (as for the O ions).

Consider now the situations with S_2 in the capping layer (full layer):

Without Co



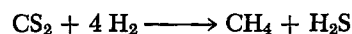
With Co



(For simplicity, only the monolayer and capping layer are shown.) Cases Ic2 and IIc2 are illustrated in Figures 15a and b. It is clear that the S ions block access to the Mo ions. The capping layer of the catalyst accordingly should contain extra anion vacancies where S^{2-} ions are removed with simultaneous reduction of the underlying Mo ions. Results of the removal of a S ion are shown in the figures; in case Ic2 an isolated Mo^{3+} ion is left, and in case IIc2 a pair of Mo^{3+} ions is left. Case IIc1 is similar to its Co-containing counterpart, but the structure for case Ic1 cannot be reduced to give Mo^{3+} .

If we postulate that an active layer must contain Mo^{3+} (in agreement with Voorhoeve), and further that a stable monolayer must contain Al, then the promoter action of Co is explained: Co increases the reduction of Mo while secondarily (but still significantly) stabilizing the monolayer. Intercalation into the disulfide and incorporation into the support therefore serve the same purpose—the reduction of Mo. It is interesting that the intercalation model then stresses the preference of the promoter for an octahedral site, and the incorporation model its preference for a tetrahedral site.

Catalytic Behavior of the Ni/W System. The experimental investigations of catalytic properties of the Ni/W system are entirely due to Voorhoeve and Stuiver (1971a, b) and to Farragher and Cossee (1972). Voorhoeve and Stuiver investigated the hydrogenation of cyclohexene and benzene. To maintain a steady state sulfur content they added CS_2 to the feeds, and this was converted to CH_4 :



The reactions were followed with a microflow technique for the following ranges of variables: $P = 4.8 \times 10^6 \text{ N/m}^2$; $P_{\text{H}_2}:P_{\text{HC}} = 35$; $T = 473 \text{ to } 673^\circ \text{K}$; $\text{SV} = 4 \text{ to } 1000 \times 10^{-3} \text{ m}^3 \text{ liquid/kg of catalyst/sec}$. Conversions were as follows: Benzene and cyclohexene, 1 to 95%; CS_2 , always 100%.

The benzene hydrogenation followed first order kinetics while hydrogenation of cyclohexene was first order in the olefin concentration; both reactions were inhibited by H_2S . Arrhenius plots for benzene and cyclohexene hydrogenation were curved. The kinetic equations for the two reactions were similar for bulk sulfides and commercial BASF 0376 catalyst (22.6 wt. % W and 3.8 wt. % Ni as

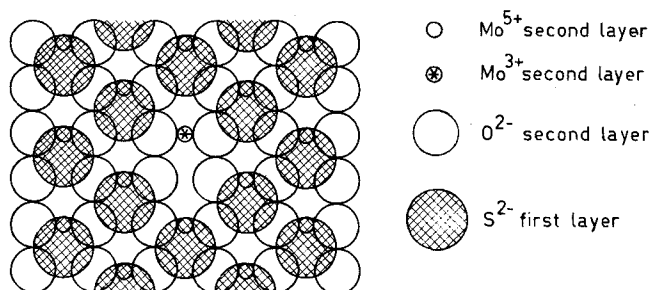


Fig. 15a. Sulfided monolayers on Co-promoted $\gamma\text{-Al}_2\text{O}_3$: Surface layer is a C-layer.

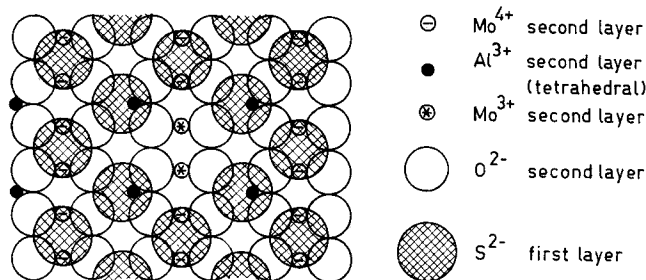


Fig. 15b. Sulfided monolayers on Co-promoted $\gamma\text{-Al}_2\text{O}_3$: Surface layer is a D-layer. Sulfur layers are depicted to be as dense as possible except for single sites at which a sulfur anion vacancy exists. These sites are suggested as the catalytically active sites.

sulfides supported on alumina; surface area was $1.43 \times 10^5 \text{ m}^2/\text{kg}$. The relative rates of reaction were 8.3 and 100 for hydrogenation of benzene and cyclohexene, respectively.

Figure 16 shows the promoter action of Ni on a bulk WS_2 catalyst for the hydrogenation of cyclohexene; the

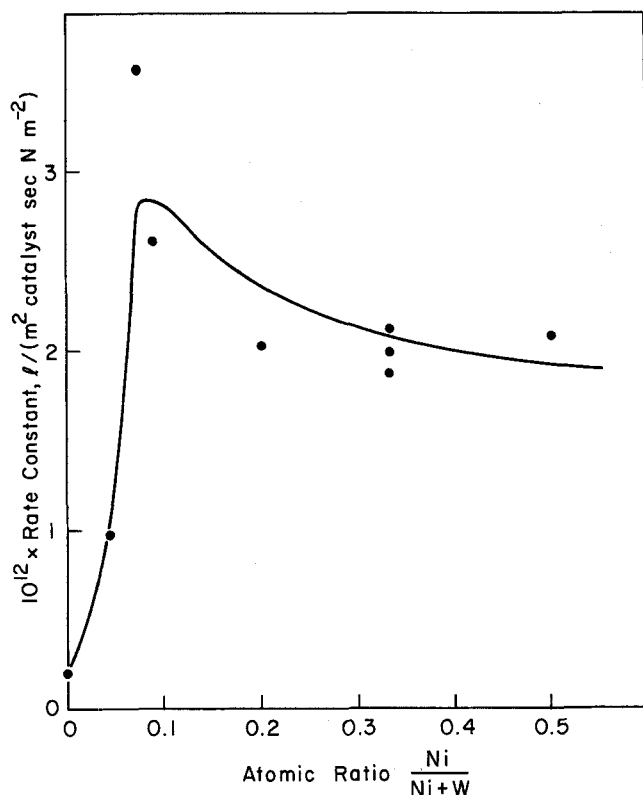


Fig. 16. Effect of Ni:W atomic ratio in Ni/W/S catalyst on rate of hydrogenation of cyclohexene at 559°K (Voorhoeve and Stuijver, 1971b).

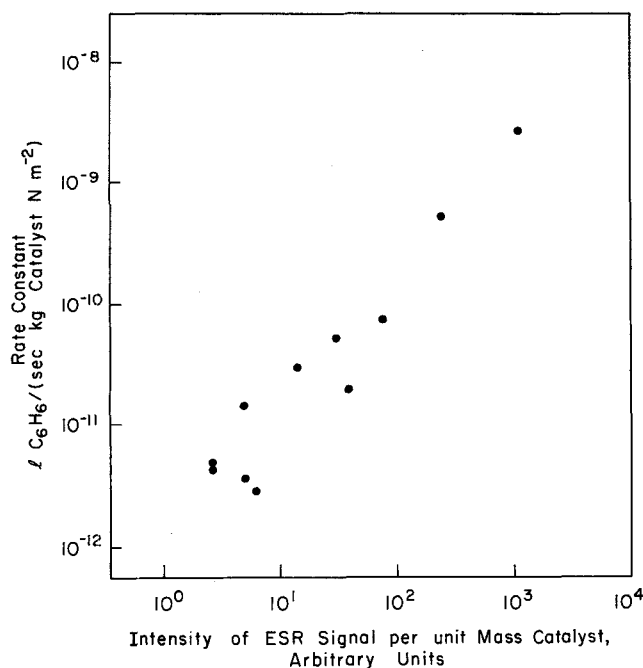


Fig. 17. Correlation of catalytic activity for benzene hydrogenation with intensity of tungsten ESR signal (Voorhoeve, 1971).

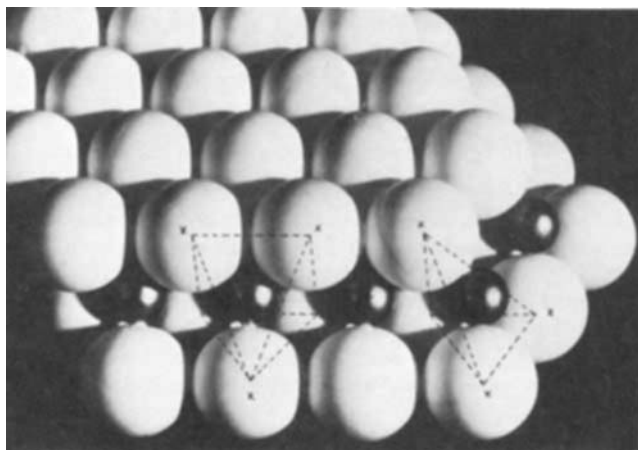


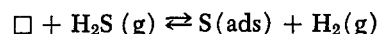
Fig. 18. Model of small WS_2 crystallite: white spheres represent sulfur ions; black tungsten. Steric hindrance of adsorption is caused by sulfur ions marked by crosses (Voorhoeve and Stuijver, 1971b).

rate increased 15-fold as the atomic fraction Ni increased from 0 to 0.1.

At higher Ni concentrations there was a decrease in the promoter action. The promoter action was much stronger for the benzene hydrogenation on both supported and unsupported catalysts; the $\text{Ni}_{0.5}\text{WS}_2$ catalysts were 200 times more active than WS_2 . Here too the first added Ni had the greatest effect.

The rate constant for benzene hydrogenation was correlated over several orders of magnitude with intensity of the ESR signal assigned to W^{3+} (Figure 17). No correlation was found between the activity of the catalyst in cyclohexene hydrogenation and the intensity of the ESR signal.

These results led Voorhoeve and Stuijver to propose two different catalytic sites (one for cyclohexene and the other for benzene hydrogenation). Both are situated on the edges of the WS_2 layers. They are W^{3+} ions in a coordination derived from the trigonal prismatic when one or two of the anion sites is left vacant. Evidence that these are actually present is the result that both reactions are inhibited by H_2S , presumably because of the interaction



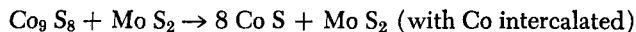
where \square is an anion vacancy.

The manner in which these vacancies arise is shown in Figure 18.

Farragher and Cossee proposed a refined interpretation of these site structures based on electron microscopic observations of a rounding of the WS_2 edges after introduction of Ni. The authors considered the two sites to be a single W^{3+} ion connected to a vacancy and a combination of two W^{3+} ions with interconnecting S^{2-} ions absent.

Catalytic Behavior of the Co/Mo System. Voorhoeve and Stuijver and Farragher and Cossee suggested that their models would be valid for Mo- as well as W-sulfides, although no experimental confirmation was presented for a Mo-sulfide system. CoMo_2S_4 might be considered to be an ideal intercalation compound, yet it was found by Hagenbach et al. (1971a, b) to be almost inactive as a catalyst. This result is ascribed by Farragher and Cossee to the different type of S-coordination (octahedral instead of trigonal prismatic). It is difficult to understand, however, why this difference should play such a vital role in the behavior of the surface sites which are anion-deficient.

On the other hand, Hagenbach et al. found a combination of $\text{Co}_9\text{S}_8 + \text{MoS}_2$ to have somewhat higher activity than MoS_2 alone. This might perhaps be explained by a reaction such as



Data showing the effects of structure of supported catalysts on hydrosulfurization of model compounds are scarce. Recent work at Eindhoven and Carleton University, Ottawa, led to a report by de Beer et al. (to be published) on the conversion of thiophene at 673°K and $1.0 \times 10^5 \text{ N/m}^2$ on various catalysts of the type $\text{MeO}/\text{MoO}_3/\text{Al}_2\text{O}_3$ (with $\text{Me} = \text{Mn}^{2+}, \text{Co}^{2+}, \text{Zn}^{2+}$). A comparison was also made with commercial Co/Mo

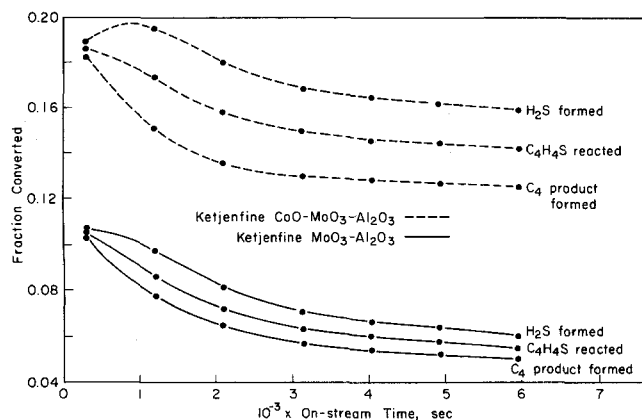


Fig. 19. Hydrosulfurization of thiophene in a flow reactor. Catalyst ($1.8 \times 10^{-4}\text{kg}$) reduced in H_2 for $5.4 \times 10^3 \text{ sec}$. at 673°K . Feed: $9.5 \times 10^{-7} \text{ m}^3\text{H}_2$ at STP/sec. + 6 vol% thiophene at 673°K (de Beer et al., in press).

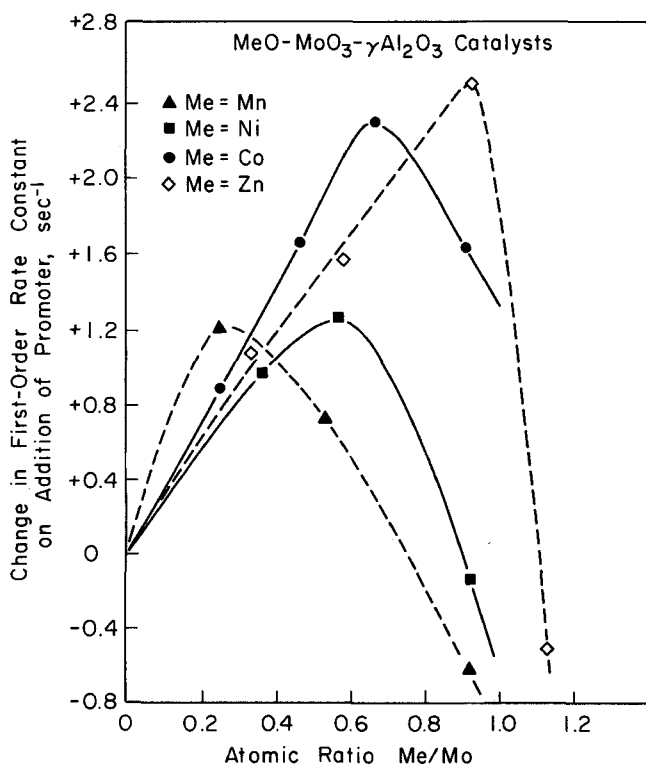


Fig. 20. Dependence of rate of thiophene hydrosulfurization on catalyst promoter concentration. Catalyst ($1.8 \times 10^{-4}\text{kg}$) reduced in H_2 for $5.4 \times 10^3 \text{ sec}$. at 673°K . Feed: $24 \times 10^{-6} \text{ m}^3 \text{H}_2$ at STP/sec. + 6 vol% thiophene at 673°K (de Beer et al., in press).

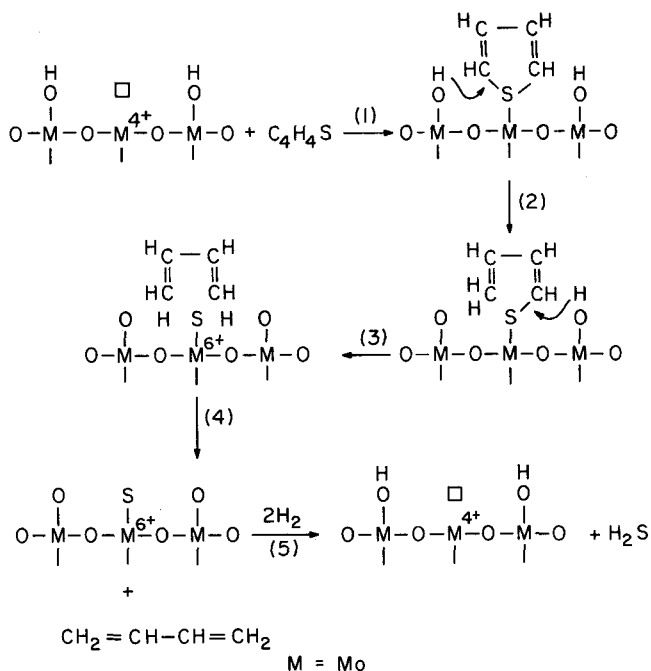


Fig. 21. Postulated mechanism for hydrosulfurization of thiophene (Lipsch and Schuit, 1969c).

catalysts from Ketjen. All catalyst were reduced by H_2 at 673°K prior to reaction.

Figure 19 gives a survey of a typical run: conversion was initially relatively high with the oxide catalyst, then it declined to a steady state level. The value of the steady state conversion is plotted versus the promoter concentration in Figure 20. Conversion passed through a maximum with increasing promoter concentration. The initial increase was the same for all promoters, but the position of the maximum increased in the order $\text{Mn}^{2+} \approx \text{Ni}^{2+} < \text{Co}^{2+} = \text{Zn}^{2+}$.

Mn^{2+} in the catalyst has no preference for tetrahedral or octahedral sites; Ni^{2+} prefers octahedral sites but at low concentrations is present in the tetrahedral sites (Lo Jacono et al., 1971); and Co^{2+} and Zn^{2+} prefer tetrahedral sites. The tendency to occupy tetrahedral positions therefore appears to be important in making a metal cation a promoter. Although there is no question that the catalyst became partially sulfided during the conversion, activity was not limited to sulfides; the reduced oxide systems invariably showed activity.

Lipsch and Schuit (1971a, b, c) suggested that the catalytically active site was Mo^{4+} in an octahedral coordination with some vacancies in place of oxygen. The postulated reaction mechanism for thiophene is given in Figure 21.

Lipsch did not give an explanation of the promoter action of Co^{2+} . The model given in Figure 15b is an attempt in this direction which moreover accounts for the partial sulfiding. Consequently, Lipsch's proposal can be modified. The active site is now envisioned to be a combination of four Mo^{3+} ions, two of which are associated with (SH) - groups arising from the reaction



The other Mo^{3+} ions are the pair associated with the anion vacancy (compare Lipsch's three Mo^{4+} and two $(\text{OH})^-$).

The reaction, just as in Lipsch's proposal, is a concerted process in which the hydrogen atoms are donated to the thiophene molecule that donates its sulfur atom

TABLE 12. DISTILLATE HYDRODESULFURIZATION PLANTS (LISTER, 1965)

Location	Approx. design date	Process variables				Catalyst bed details			Reactor details			
		$10^3 \times$ throughput m ³ oil/sec. ^{**}	$10^4 \times$ space velocity vol. oil/sec./vol. catalyst	$10^{-6} \times$ pressure, N/m ²	Temp., °K	Recycle gas rate, std. m ³ /m ³ oil	Diam., m	Depth, m	Volume, m ³	Vessel I.D., m	Tangent length, m	Type of construction [‡]
Kwinana	1952	11.5	22.2	6.9	689	720	1.2	4.2	4.6	1.2	5.2	A
Hamburg	1954	13.3	3.8	4.7	639-655	260	2.0	9.9 [*]	31.4	2.0	11.9	B
Kent (Nos. 1 and 2)	1955	20.4	8.3	4.2	661-689	450	1.8	2.7	7.0	2.0 ⁺	3.4	C
Antwerp												
Venice	1957	13.3	11.1	3.6	689	360	1.6	5.4	11.0	1.6	6.8	B
Ruhr	1958	20.4	22.2	6.9	689	180	1.8	3.6	8.6	1.9	4.3	C
Belfast	1961	7.8	22.2	6.9	694	180	1.4	2.3	3.4	1.4	3.2	D
Lavera	1962	30.7	11.1	3.6	694	360	2.2	6.6	25.3	2.5	6.7	C

^{**} Data of Lister were given in units of bbl/std. day. One std. day was assumed to be 7.76×10^4 sec.

^{*} 3 beds, each 3.3m deep.

⁺ 3 identical reactors in series on each unit (total catalyst volume 21 m³).

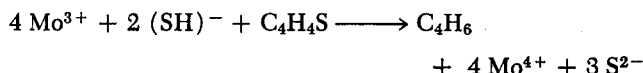
[‡] Construction A. Solid stainless steel (18/8/Ti).

B. Clad Plate: 18/8/Ti on C/½ Mo.

C. C/½ Mo. Vessel with refractory lining + 18/8/Ti shroud.

D. Clad Plate: 18/8/Ti on 1 Cr/½ Mo.

to the anion vacancy, thus producing butadiene:



The product butadiene is subsequently hydrogenated; whether this occurs on the same site or one of a second kind is not known. Figure 15a contains a suggestion of a second kind of site, the isolated Mo^{3+} ion. There is doubt of the existence of this site, and if it is present at all, its concentration is probably low. Because of its similarity to Voorhoeve's single type of site, it might be expected to have hydrogenation properties, though for now the suggestion is only speculation.

Conclusions

There are now two proposed structures which might be held responsible for the activity of hydrodesulfurization catalysts: on the one hand, the trigonal prismatic MoS_2 and WS_2 systems intercalated by the promoter ions because of defects originating at layer edges; on the other hand, the surface layer of the support containing Mo or W and stabilized by the presence of promoter ions in tetrahedral sites in the support. The former structure, for the special case of $\text{Ni} + \text{WS}_2$, has been shown to be an active hydrogenation catalyst. The latter fits the Co/Mo system better and has been shown to be a hydrodesulfurization catalyst for thiophene even in the reduced state.

The statement that there are alternative proposals for the catalyst structure may be misleading. Possibly the two systems are present simultaneously and operate in combination. For example, the monolayer structure might form butadiene from thiophene while the intercalated system hydrogenates it further to butene. For more complicated molecules such as the benzothiophenes studied by Givens and Venuto, the sequence might be reversed, hydrogenation followed by desulfurization. Perhaps commercial catalysts are necessarily bistructural in order to maximize the intrinsically bifunctional operation.

An especially interesting case in this connection is represented by the $\text{NiO}/\text{MoO}_3/\text{Al}_2\text{O}_3$ system, which we have hardly discussed because there are so few data, even though it is reputed to be an active and perhaps industrially applied catalyst. Ni as a promoter seems to fit better in the intercalated sulfide model than in the mono-

layer model. More extensive studies of $\text{NiO}/\text{MoO}_3/\text{Al}_2\text{O}_3$ as compared to $\text{CoO}/\text{MoO}_3/\text{Al}_2\text{O}_3$ catalysts might therefore lead to a better appreciation of the catalytic mechanism in hydrodesulfurization.

PROCESS DESIGN

A general description of hydrodesulfurization processes was given earlier. Details of light distillate processes are given in reviews by Docksey and Gilbert (1967) and Schuman and Shalit (1970). An account given by Lister (1965) concerns commercial operating experiences, including details of reactor design, construction, and operation. Some of Lister's data are collected in Table 12. Conversions of sulfur were not given, but they were surely less than conversions in modern units which are required to provide catalytic reformer feeds containing only a few tenths of a part per million of sulfur, corresponding to conversions of as much as 99.97%.

The following section emphasizes engineering considerations for hydrodesulfurization of heavier feeds (gas oils and residua). Since these feeds present the greater and more recently recognized engineering challenges, the related literature is far less developed. Our intention is to identify engineering problems and to evaluate their importance in process design. Frequently, the evaluations will be superficial and speculative since there are few quantitative data available. The data to be presented as examples should not always be considered representative of commercial practice.

Separation Processes

In hydrodesulfurization processes the product purification procedures are well established. Gaseous and liquid products are separated at high pressure in a single stage, and the oil is stripped to remove remaining dissolved light products. The hydrogen stream from the phase separator is scrubbed with monoethanolamine, for example, to remove hydrocarbon and H_2S , which inhibits reaction.

Standard operating procedure appears to always include scrubbing of H_2S from hydrogen recycle streams. Scrubbing of interstage reactor streams may also be practiced; an alternative procedure for interstage purification involves selective adsorption of H_2S on zinc oxide (Phillipson, 1971).

The ease of separation of fluid-phase reaction products from solid catalyst is a strong advantage of fixed-bed reactor designs. In the slurry-bed processes, small particles of catalyst may be continuously removed with products. Problems with filtration are to be expected, and plugging of filters may be difficult to avoid.

Mass Transfer Effects

A number of authors have reported experiments with trickle-bed hydrodesulfurization at constant space velocity and varying mass velocities. For example, Cecil et al. (1968) reported pilot plant experiments with several distillates, heavy vacuum gas oils, and residua, finding no effect on reaction rate of changes in mass velocity of oil in the range of about 0.13 to 0.54 kg/m²/sec. A representative particle dimension was probably about 3×10^{-3} m. It appears to be safe to conclude that external-phase mass transfer does not influence rates of hydrodesulfurization in well designed pilot-scale reactors. Since mass velocities are almost always greater in commercial scale reactors, the external-phase resistances in them are also expected to be negligible.

In contrast, mass transfer resistance within catalyst pores appears to be significant for feeds ranging from light distillates to residua. Rates of transport of either hydrogen or sulfur-containing oil molecules in liquid-filled pores may be low compared to intrinsic rates of reaction. It is useful to account for the effects with the Thiele model for diffusion and first-order isothermal reaction in porous catalyst particles (van Deemter, 1965).

The standard experimental test for a significant intraparticle mass transfer resistance is a series of reaction rate determinations with catalyst particles of various sizes and otherwise constant operating conditions. As van Deemter (1965) has pointed out, a perfectly mixed stirred-tank reactor is most appropriate for obtaining such data, since reaction rates can be determined directly at any conversion. The catalyst may best be contained in a spinning basket (Carberry reactor).

Adlington and Thompson (1965) estimated that effectiveness factors for hydrodesulfurization at 688°K and 3.5×10^6 N/m² were about 0.6 for 3.2×10^{-3} m-diameter pelleted catalyst. Their estimates showed that effectiveness factor did not change appreciably with feed boiling range (the range was unspecified), suggesting that the decreased reactivities of the heavier sulfur compounds were roughly compensated by their decreased diffusivities.

Effects of catalyst particle size on rates of hydrodesulfurization of Middle Eastern residua were measured by le Nobel and Choufour (1959) and Cecil et al. (1968). The latter authors found an effectiveness factor of 0.4 for cylindrical particles 1.6×10^{-3} m in diameter; when the average pore diameter was increased from 7.8 to 10.3 nm, the estimated effectiveness factor increased to 0.8.

Even though there are only few data, it appears to be safe to generalize: effectiveness factors in hydrodesulfurization are slightly less than one for many feeds and catalysts. The right-hand side of Equation (7) should be multiplied by an effectiveness factor; it is recommended that values of effectiveness factor be determined experimentally for each catalyst and feed. Systematic experimental studies of the intraparticle mass transfer effects in hydrodesulfurization would be valuable additions to the literature.

The effectiveness factor may be subject to significant change during catalyst aging, as is to be discussed later; another important intraparticle mass transfer effect involves the demetallization reactions associated with catalyst aging, which will also be discussed later.

TABLE 13. TYPICAL FEEDSTOCK INSPECTIONS (CECIL ET AL., 1968)

	Middle Eastern		Venezuelan	
	Residuum	Gas oil	Residuum	Gas oil
Specific gravity	0.96	0.93	0.95	0.91
Sulfur, wt. %	4.01	2.95	2.17	1.56
Conradson carbon, wt. %	12.2	0.37	10.7	0.28
Naphtha insolubles, wt. %	9.6	0.4	10.0	—
Carbon, wt. %	84.52	85.20	85.93	—
Hydrogen, wt. %	11.05	11.79	11.43	—
Nickel, ppm	27	0.3	37	0.7
Vanadium, ppm	76	0.4	290	0.7
ASTM distillation (Atm. Equiv.), °K				
5%	599	650	588	658
10%	629	684	622	665
20%	675	708	670	678
40%	757	731	753	704
60%	830	753	831	741
90%	—	783	—	794

Fluid Flow and Mixing Effects

Cecil et al. (1968) reported experiments with pulses of radioactive dotriacontane (C₃₂H₆₆) tracer, which were designed to determine the residence time distribution of oil in 2.5×10^{-2} m-diameter trickle-bed reactors. Catalyst particle size was not specified; it is assumed the catalyst particles were cylinders, about 1.6 to 3.2×10^{-3} m in diameter. Though deviations from piston flow were observed, the authors concluded that they had negligible effect on typical conversions of gas oil at liquid mass velocities ranging from 4.7×10^{-2} to 2.0 kg/m²/sec.

In commercial-scale trickle-bed reactors, however, deviations from piston flow of liquid are much more difficult to avoid, and reactor efficiency may be much less than that experienced with the same catalyst in a pilot-scale reactor (Ross, 1965). Ross and Cecil et al., among others, have emphasized the need for design to give even distribution of liquid in commercial-scale trickle-bed reactors. Lister (1965) recommended a perforated plate/chimney type distributor for gas-liquid feeds to each reactor stage employed. Although practical design details are not available in the open literature, we infer that piston flow has been closely approached on a routine basis with proper distributor design.

Initial estimates of axial mixing effects might best be based on correlations representing data from laboratory-scale reactors. The recent literature includes papers by Hochman and Efron (1969), van Swaaij et al. (1969), and Mears (1971).

In the prospective absence of deviations from piston flow and external-phase mass transport resistance, Equation (7), the recommended rate equation, can be integrated straightforwardly to give optimistic reactor design estimates, provided methods are available to account for catalyst aging.

The distribution of flow in slurry-bed hydrodesulfurization reactors is not well characterized. It is probably a good first approximation that the oil and catalyst are perfectly mixed in the reactor. The hydrogen flowing through the slurry as bubbles might be nearly in piston flow.

The consequences of this mixing of reacted and un-

reacted compounds are clear. For example, for a second-order reaction in a perfectly mixed reactor, the required reactor volume is roughly twice that of a piston-flow reactor at 40% conversion and about five times that of a piston-flow reactor at 80% conversion. Reactor volume in the slurry-bed process can be significantly reduced if multiple stages are used. High temperature reactors and consequently higher reaction rates can also be used; this option is probably most desirable when processing objectives include hydrocracking of residua.

The design of flow distributors is undoubtedly of importance in the fluidized-bed process. Even distribution of gas bubbles in the bed and avoidance of slugging are essential to maintenance of fluidization and even temperature distribution; mechanical recirculation of oil may be employed to provide sufficient velocity for fluidization of larger catalyst particles (Mounce and Rubin, 1971).

Catalyst Aging

Some of the unique engineering problems associated with hydrodesulfurization of residual petroleum fractions are consequences of the presence of organometallic compounds contained primarily in the heaviest (asphaltene) fraction of the residuum. Feedstock inspections of a Middle Eastern and of a Venezuelan residuum are compared to the inspections of the corresponding gas oils in Table 13. The V and Ni are almost completely contained in the residual fraction, while the sulfur is almost evenly distributed. The Venezuelan residuum contains about 330 ppm V plus Ni.

The nature of V and Ni compounds in petroleum has

been discussed by Larson and Beuther (1966). Metals in the asphaltene fraction are believed to be present as organometallic compounds associated in the form of micelles. A schematic representation of such a micelle is shown in Figure 22. A micelle is 4 to 5 nm in diameter, too large to pass through many of the pores in practical hydrodesulfurization catalysts (Table 14).

Removal of V is generally found to be more rapid than removal of Ni. For example, Hiemenz (1963) found that inorganic V was deposited within the pores of catalyst particles used to hydrodesulfurize an Iranian topped

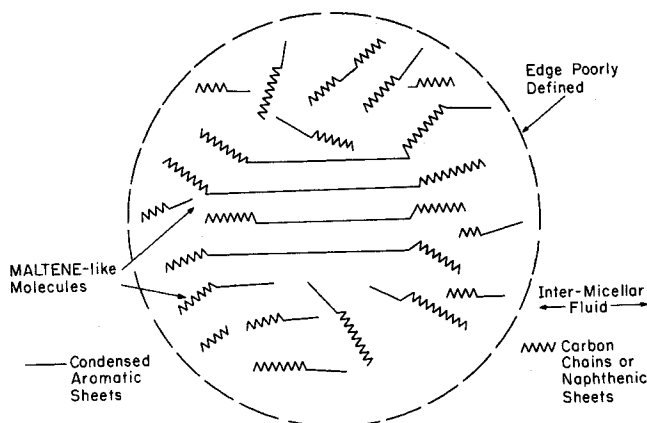


Fig. 22. Schematic depiction of an asphaltene micelle (Larson and Beuther, 1966).

TABLE 14. CATALYSTS FOR HYDROTREATING OF RESIDUA (VLUGTER AND VAN'T SPIJKER, 1971)

Manufacturer	Preferred metals	wt. % SiO ₂ in silica alumina; (plus other components)	10 ⁻³ × bulk density, kg/m ³	10 ³ × avg. pore volume, m ³ /kg	Avg. pore diam., mm	10 ⁻⁵ × specific surface area m ² /kg
Esso	Ni + Mo or Co + Mo	1-6	<0.70	>0.25	mainly 3-7	>1.5
UOP	Ni + Mo	10-40	0.625-0.875	0.3-0.5	6-10	1.5-2.5
Standard Oil Ind.	Co/Mo*	pref. 10-25 pref. 1-10	—	>0.5	10-20	1.5-5 pref. 3-3.5
Gulf	Mo + Co + Ni	0	—	0.46	regular distribution 0-24; avg. diam. 14-18	1.6-2.2
Texaco	Ni or Co + Mo or Ni + W	2-30	0.5-0.7	0.6-0.8	—	3-8
UOP	Ni + Mo	10-90 (+ boron phosphate ±)	0.15-0.35	1.23	12.5	—
Shell	Ni/Co-W/Mo	pref. 70 to 90	0.71	—	9	2.9
Chevron	Group VI + VIII	SiO ₂ practically none (+ metal phosphates)	—	porosity >60%	>6	>1
Nippon Oil Co.	Co/Mo or Ni/W	0	—	0.3 of pores >7.5 nm	many pores of 100-5,000	—
Hydrocarbon Research	Co/Mo (+ Ni)	0-100	—	0.45-0.5	6-7 plus channels 10-100 plus channels > 100	2.6-3.6
Commercial Samples						
Girdler G-35B	Co/Mo	—	0.96	0.22	mainly <20	2.7
Pro Catalyse Co.	Co/Mo	—	0.5	0.78	regular distribution up to 1,000 plus larger pores	2.8
IFD HR 304					peak at 40	
Davison Chemical Co.	Ni/Co/Mo	—	0.64	0.39		2.2
NiCoMo-1						

* May contain zeolites.

± Boron phosphate probably provides mechanical strength to catalysts of low density.

residuum; the V was concentrated near the particle peripheries in sharply defined layers 1.3×10^{-4} m thick. The outer layers included only about 8% of the catalyst pore volume. Hiemenz found that deposited Ni was more uniformly distributed in the catalyst particle, occupying the outer 18% of the particle volume; the distribution of deposited carbon (coke) was uniform in the particle. Hiemenz showed that oxidized catalyst material containing the inorganic V and Ni offered greater resistance to intraparticle mass transport than the uncontaminated material. It is clear that under some circumstances the deposition of Ni and especially V within the pores of hydrodesulfurization catalysts can lead to restriction of the diffusion paths of reactant molecules and ultimately to blocking of these paths and irreversible deactivation of the catalyst.

The occurrence of this pore-blocking phenomenon indicates the advantage of catalysts with large pores and increased pore volume to provide easy access and high capacity for the inorganic metal compounds. Trade-offs in the catalyst design are clear: larger pores and increased pore volume can be obtained at the expense of small pores and surface area, hence at the expense of intrinsic catalyst activity. Pore volume increases obtained through increased catalyst porosity produce particles of decreasing mechanical strength. An aged residuum hydrodesulfurization catalyst with a loading of more than 0.5 kg Ni plus V per kg catalyst was reported by Paradis et al. (1971).

The research problems associated with blocking of pores and the diffusion of large molecules in small pores are deserving of attention. The mass transport phenomena are complex, involving the slow motion of molecules which interact strongly with pore walls and which may have to deform to pass through narrow passages; the transport of large hydrocarbon molecules in pores of alumina-based materials may be comparable to the transport of smaller molecules in the intracrystalline channels of zeolites.

Moritz et al. (1971) reported that with an unidentified conventional catalyst used in hydrodesulfurization of

Kuwait atmospheric residuum, fractional removal of Ni plus V was roughly the same as fractional removal of sulfur. With an unspecified improved catalyst, only about half this degree of metal removal was observed; consequently, catalyst aging was less rapid, and the amount of sulfur removed before catalyst replacement was increased.

These results suggest that a catalyst with molecular-sieving properties has been prepared. If most of the pores had diameters of about 4 nm or less, the metal-containing asphaltenes would be sieved out while most of the sulfur-containing molecules could enter the catalyst pores and penetrate toward the particle interior (though effectiveness factors might be small). There is fruitful ground for research into methods of tailoring the physical properties of alumina-based catalysts.

It is conceivable that zeolites have been used to catalyze hydrodesulfurization reactions; the use of shape-selective (zeolite) catalysts for hydrocracking reactions has been reported, for example, in a patent by Arey et al. (1966). They described a two-stage residuum hydrocracking process—in the first stage, metals and other contaminants were partially removed by reaction catalyzed by cobalt molybdate having an average pore diameter of 8 nm; in the second stage, a palladium-loaded zeolite with a pore diameter of 1.3 nm selectively catalyzed further reaction of the smaller molecules, sieving out large metal-containing molecules which otherwise would react to form deposits of inorganic metals and coke.

Although accumulation of inorganic material within catalyst pores causes an irreversible loss of catalyst activity, the simultaneous accumulation of coke does not, and regeneration by controlled oxidation is standard practice, at least in operation with light feeds. For example, van Deemter (1965) observed a rapid decline in activity of cobalt molybdate after about 1.5×10^7 kg of gas oil had been hydrodesulfurized per m^3 of catalyst bed. The catalyst then contained 5.2 wt. % coke. The catalyst regained full activity when the carbon was burned off under carefully controlled conditions. The rapid activity loss was perhaps indicative of pore blocking by coke.

The deposition of solids in fixed-bed interstices also presents significant engineering problems. Lister's account (1965) cites uneven distribution of flow and excessive pressure drop resulting from deposition of solids at the upstream end of a fixed-bed reactor. Feed contamination with sodium chloride must be avoided, as salt deposits form rapidly. Lister recommended mesh baskets at the top of a fixed-bed reactor. These should contain loosely packed solids, providing high interstitial capacity for deposited material. The baskets could be replaced periodically. A separate guard chamber operated as a swing reactor upstream of the main reactor could serve the same purpose.

Data of Kubička et al. (1968) demonstrate the usefulness of a guard chamber. In pilot-scale fixed-bed hydrodesulfurization of Romashkino residuum, the solid deposits (especially iron and scale) were concentrated near the bed entrance; V was more strongly concentrated near the entrance than Ni, corresponding to the greater reactivity of organovanadium compounds. Newson (1972) has inferred from the literature that the major source of interstitial deposits is the organometallic components of residua, but Weekman (1972) cited unpublished operating data showing that scale and corrosion products, not V and Ni, predominate in the deposits. The available data do not allow resolution of the disagreement.

An advantage of the slurry-bed reactor is the continuous removal of solid material formed in reaction. Presumably this material must be separated from the catalyst.

TABLE 15a. OPERATING CONDITIONS FOR COST STUDY
(DOCKSEY AND GILBERT, 1967)

Feed rate, m^3/sec .	4.1×10^{-2}
Feed sulfur, wt %	1.2
Product sulfur, wt %	0.1
Space velocity, vol. feed/vol. catalyst/sec.	2.2×10^{-3}
Pressure, N/m^2	6.9×10^6
Reactor temperature, $^{\circ}\text{K}$	661-694
Gas recycle rate, std. $\text{m}^3 \text{H}_2/\text{m}^3 \text{oil}$	180
Hydrogen consumption, std. $\text{m}^3 \text{H}_2/\text{m}^3 \text{oil}$	32

TABLE 15b. COST SUMMARY FOR LIGHT DISTILLATE
DESULFURIZATION PLANT (DOCKSEY AND GILBERT, 1967)

Duty	Cost, $\text{¢}/\text{m}^3$ product			% of total cost
	Capital charges	Chemicals and utilities	Total cost	
Feed to reaction condition	14.5	18.1	32.6	54
Hydrogen to reaction condition	3.5	2.6	6.1	10
Gas circulation	5.8	3.9	9.7	16
Reactor and catalyst	2.4	1.9	4.3	7
Product recovery	6.6	1.6	8.1	13
Total	33	28	61	100

Reactor Stability

The heat of reaction of residuum hydrodesulfurization is sufficient to raise the reactant temperature about 20 to 80°K at typical operating conditions (Mounce and Rubin, 1971); to compensate for the temperature rise in fixed-bed reactors, cold hydrogen may be added between stages. Nonetheless, the occurrence of hot spots in hydrodesulfurization reactors has been repeatedly cited, for example, by Lister (1965), who identified the hot spots as a symptom of catalyst aging causing poor flow distribution. It is possible that uncontrollable temperature excursions could occur in fixed-bed reactors since highly exothermic side reactions like hydrocracking begin to take place rapidly at temperatures not much higher than normally encountered.

Instability would seem to be less likely for the back-mixed slurry-bed reactors since heat transfer is rapid; the maximum temperature difference between any two points in a reactor is reported to be normally less than 3°K (Mounce and Rubin, 1971). Yet a commercial-scale slurry-bed hydrodesulfurization reactor is known to have exploded (Anonymous, 1970; Davis, 1972), and we may speculate that the explosion resulted from localized overheating in the reactor. Such overheating would have resulted if fluidization had not been maintained at some location in the reactor. The potential hazard points to a clear need for operating data and analysis of the instability phenomena.

Process Economics

Docksey and Gilbert (1967) summarized costs of hydrodesulfurization of light distillates. Their estimates (Table 15) are probably still representative. The costs of such processes are not sensitive to the reactor design (Lister, 1965). There seems to be little expectation of much immediate improvement in these well established processes.

Technology of hydrodesulfurization of residual fractions is developing rapidly, however, and the economics cannot be summarized easily. The number of commercial units is small (about five) but increasing, and the trend in the literature suggests a general preference for fixed-bed over fluidized-bed reactors. The processing costs are sensitive to feed properties (such as content of metals), the cost of hydrogen, and the evolving air quality standards. In a recent review of the process development literature, Ebel (1972) cited some processing costs and alternative routes to low-sulfur fuel oil.

NOTATION

c	= concentration, wt. %
k	= reaction rate constant
K	= adsorption equilibrium constant
$LHSV$	= liquid hourly space velocity
P	= pressure; partial pressure
r	= reaction rate
SV	= space velocity
T	= temperature
α_1	= fraction of sulfur which is reactive
α_2	= fraction of sulfur which is unreactive

Subscripts

B	= butene
HC	= hydrocarbon
HDS	= hydrodesulfurization
Hyd	= hydrogenation
o	= feed; octahedral
S	= sulfur-containing compound or sulfur

t	= tetrahedral
T	= thiophene

LITERATURE CITED

- Adlington, D., and E. Thompson, "Desulphurization in Fixed and Fluidized Bed Catalyst Systems," in *Third European Symp. on Chem. Reaction Eng.*, pp. 203-213, Pergamon Press, Oxford (1965).
- Anonymous, "Bayway Blast, Strike Pose Fuels Threat," *Oil Gas J.*, **68** (50), 50 (1970).
- Arey, W. F., R. B. Mason, and R. C. Paule, "Process for Hydrocracking Heavy Oils in Two Stages," U.S. Pat. 3,254,017 (1966).
- Ashley, J. H., and P. C. H. Mitchell, "Cobalt-Molybdenum-Alumina Hydrodesulfurization Catalysts. Part I. A Spectroscopic and Magnetic Study of the Fresh Catalyst and Model Compounds," *J. Chem. Soc., A*, 2821 (1968).
- , "Cobalt-Molybdenum-Alumina Hydrodesulfurization Catalysts. Part II. Incorporation of Cobalt (II) and Molybdenum (VI) into γ -Alumina," *ibid.*, 2730 (1969).
- Asmolov, G. N., and O. V. Krylov, "Investigation of Molybdenum Oxide Catalysts on γ - Al_2O_3 and MgO with the Aid of the Diffuse Reflection Spectra," *Kinet. Katal. (Engl.)*, **11**, 847 (1970).
- Beuther, H., and B. K. Schmid, "Reaction Mechanisms and Rates in Residual Hydrodesulfurization," in *Proc. Sixth World Petrol. Congress, Sect. III*, p. 297, Verein für Förderung des 6-Welt-Erdöl Kongresses, Hamburg (1964).
- Cecil, R. R., F. X. Mayer, and E. N. Cart, "Fuel Oil Hydrodesulfurization Studies in Pilot Plant Reactors," paper presented at Am. Inst. Chem. Engrs. Meeting, Los Angeles (1968).
- Chevreil, R., M. Sergent, and J. Prigent, "Préparation de Thio molybdates d'Elements de Transition," *C.R. Acad. Sci. Paris, Ser. C*, **267**, 1135 (1968).
- Cossee, P., "Magnetic Properties of Co in Co_3O_4 and other Oxides," Ph.D. thesis, Univ. Leiden, The Netherlands (1956).
- Davis, J. C., "More SO_2 -from-Resid Options," *Chem. Eng.*, **36** (July 10, 1972).
- de Beer, V. H. J., T. H. M. van Sint Fiet, J. F. Engelen, A. C. van Haandel, M. W. J. Wolfs, C. H. Amberg, and G. C. A. Schuit, "The CoO - MoO_3 - Al_2O_3 Catalyst. IV. Pulse and Continuous Flow experiments and Catalysts. Promotion by Cobalt, Nickel, Zinc, and Manganese," *J. Catal.*, in press.
- Desikan, P., and C. H. Amberg, "Catalytic Hydrodesulfurization of Thiophene IV. The Methylthiophenes," *Can. J. Chem.*, **41**, 1966 (1963).
- , "Catalytic Hydrodesulfurization of Thiophene V. The Hydrothiophenes. Selective Poisoning and Acidity of the Catalyst Surface," *ibid.*, **42**, 843 (1964).
- Docksey, P., and R. J. H. Gilbert, "Advances in Desulphurization of Distillates," in *Proc. of Seventh World Petrol. Congress*, **4**, p. 153-165, Elsevier, England (1967).
- Dufaux, M., M. Che, and C. Naccache, "Electron Paramagnetic Resonance Study of Catalysts based on Molybdenum and Cerium Oxides I. Reduction Properties," *J. Chim. Phys.*, **67**, 527 (1970).
- Ebel, R. H., "Recent Advances in Fuel Desulfurization Technology," *A.C.S. Div. Petrol. Chem. Preprints*, **17** (3), C46 (1972).
- Farragher, A. L., and P. Cossee, "Catalytic Chemistry of Molybdenum and Tungsten Sulfides and Related Ternary Compounds," Preprint 98, Fifth Intern. Congr. on Catal., Palm Beach (1972).
- Frye, C. G., and J. F. Mosby, "Kinetics of Hydrodesulfurization," *Chem. Eng. Progr.*, **63** (9), 66 (1967).
- Givens, E. N., and P. B. Venuto, "Hydrogenolysis of Benzothienophenes and Related Intermediates over Cobalt Molybdena Catalyst," *A.C.S. Div. Petrol. Chem. Preprints*, **15** (4), A183 (1970).
- Griffith, J. S., *The Theory of Transition Metal Ions*, p. 273, Cambridge Univ. Press, London (1961).
- Hagenbach, G., Ph. Courty, and B. Delmon, "Catalytic Activity of Cobalt and Molybdenum Sulfides in the Hydrogenolysis of Thiophene, Hydrogenation of Cyclohexene and Isomerization of Cyclohexene," *J. Catal.*, **23**, 295 (1971).

- Hagenbach, G., and B. Delmon, "Propriétés catalytiques et structurales de masses cristallisées associant le Sulfure de Molybdène MoS_2 et le Sulfure de Cobalt Co_9S_8 ," *C. R. Acad. Sci. Paris, Ser. C*, **273**, 1489 (1971).
- Hiemenz, W., in *Proc. Sixth World Petrol. Congress*, Sect. III, p. 307, Hamburg (1964).
- Hochman, J. M., and E. Effron, "Two-Phase Cocurrent Downflow in Packed Beds," *Ind. Eng. Chem. Fundamentals*, **8**, 63 (1969).
- Huisman, R., J. deJonge, C. Haas, and F. Jellinek, "Trigonal Prismatic Coordination of Solid Compounds of Transition Metals," *J. Solid State Chem.*, **3**, 56 (1971).
- Keeling, R. O., "Cobalt K Absorption Edges in Supported Cobalt-on-Alumina and Cobalt-on-Silica Catalysts," *J. Chem. Phys.*, **31**, 279 (1959).
- Kittel, C., *Introduction to Solid State Physics*, p. 550, Wiley, New York (1971).
- Kolboe, S., and C. H. Amberg, "Catalytic Hydrodesulfurization of Thiophene VI. Comparisons over Molybdenum Disulfide, Cobalt Molybdate, and Chromia Catalysts," *Can. J. Chem.*, **44**, 2623 (1966).
- Kubička, R., J. Čir, V. Novák, and J. Vepřek, "Herstellung von schwefelarmen Heizölen aus schwefelhaltigen Rohölen mit einem hohen Gehalt an metallorganischen Verbindungen aufgrund eines Beispiels von Romaschkino-Rohöl. II," *Brennst.-Chem.*, **49** (10), 308 (1968).
- Larson, O. A., and H. Beuther, "Processing Aspects of Vanadium and Nickel in Crude Oils," *A.C.S. Div. Petrol. Chem. Preprints*, **11** (2), B95 (1966).
- Le Nobel, J. W., and J. H. Choufoer, "Development in Treating Processes for the Petroleum Industry," in *Proc. 5th World Petrol. Congress*, p. 233, Fifth World Petroleum Congress, Inc., New York (1959).
- Lippens, B. C., "Structure and Texture of Alumina," Ph.D. thesis, Technical Univ. Delft, The Netherlands (1961).
- Lipsch, J. M. J. G., "The $\text{CoO-MoO}_3\text{-Al}_2\text{O}_3$ Catalyst," Ph.D. thesis, Tech. Univ. Eindhoven, The Netherlands (1968).
- , and G. C. A. Schuit, "The $\text{CoO-MoO}_3\text{-Al}_2\text{O}_3$ Catalyst I. Cobalt Molybdate and the Cobalt Oxide Molybdenum Oxide System," *J. Catal.*, **15**, 163 (1969).
- , "The $\text{CoO-MoO}_3\text{-Al}_2\text{O}_3$ Catalyst II. The Structure of the Catalyst," *ibid.*, 174.
- , "The $\text{CoO-MoO}_3\text{-Al}_2\text{O}_3$ Catalyst III. Catalytic Properties," *ibid.*, 179.
- Lister, A., "Engineering Design and Development of Desulfurizer Reactors," in *Third European Symp. Chem. Reaction Eng.*, pp. 225-235, Pergamon Press, Oxford (1965).
- Lo Jacono, M., M. Schiavello, and A. Cimoni, "Structural, Magnetic and Optical Properties of Nickel Oxide Supported on η and γ Aluminas," *J. Phys. Chem.*, **75**, 1044 (1971).
- Lo Jacono, M., J. L. Verbeek, and G. C. A. Schuit, "Electron Spin Resonance of Co-Alumina and Co-Mo-Alumina Catalysts in the Oxidized, Sulfided, and Reduced States," *J. Catal.*, in press.
- , "ESR Observation of Sulfur and Oxygen Species on Cobalt-Alumina and Moly-Cobalt-Alumina Catalysts," presented at Fifth Intern. Congr. on Catal., Palm Beach (1972).
- McKinley, J. B., in *Catalysis*, P. H. Emmett, (ed.), Vol. V, pp. 405-526, Reinhold, New York (1957).
- Mears, D. E., "The Role of Axial Dispersion in Trickle-Flow Laboratory Reactors," *Chem. Eng., Sci.*, **26**, 1361 (1971).
- Metcalfe, T. B., "Inhibition par le Sulfure d'hydrogène de la Réaction d'hydrodesulfuration des Produits pétroliers," *Chim. Ind. Gen. Chim.*, **102**, 1300 (1969).
- Moritz, K. H., H. R. Savage, D. Traficante, W. Weissman, and B. J. Young, "The CO-finishing and RESIDfinishing Processes," *Chem. Eng. Progr.*, **67** (8), 63 (1971).
- Mounce, W., and R. S. Rubin, "The H-Oil Route for Hydroprocessing," *ibid.*, 81 (1971).
- Newsome, J. W., H. W. Heiser, A. S. Russell and H. C. Stumpf, "Alumina Properties," Aluminum Co. of Am., Pittsburgh (1960).
- Newson, E. J., "Bed-Plugging due to Interparticle Reactions in Trickle-Bed Hydroprocessing," in *Chem. Reaction Eng.: Proc. of 5th European/2nd Intern. Symp. Chem. Reaction Eng.*, pp. B6-11-B6-19, Elsevier, Amsterdam (1972).
- Owens, P. J., and C. H. Amberg, "Thiophene Desulfurization by a Microreactor Technique," *Advan. Chem. Ser.*, **33**, 182 (1961).
- , "Hydrodesulfurization of Thiophene II. Reactions over a Chromia Catalyst," *Can. J. Chem.*, **40**, 941 (1962a).
- , "Hydrodesulfurization of Thiophene III. Adsorption of Reactants and Products on Chromia," *ibid.*, 947 (1962b).
- Paradis, S. G., G. D. Gould, D. A. Bea, and E. M. Reed, "Isomax Process for Residuum and Whole Crude," *Chem. Eng. Progr.*, **67** (8), 57 (1971).
- Phillipson, J. J., "Kinetics of Hydrodesulfurization of Light and Middle Distillates," paper presented at Am. Inst. Chem. Engrs. Meeting, Houston (1971).
- Richardson, J. T., "Magnetic Study of Cobalt Molybdenum Oxide Catalysts," *Ind. Eng. Chem. Fundamentals*, **3**, 154 (1964).
- Ross, L. D., "Performance of Trickle Bed Reactors," *Chem. Eng. Progr.*, **61**, (10), 77 (1965).
- Satterfield, C. N., *Mass Transfer in Heterogeneous Catalysis*, MIT Press, Cambridge, Mass. (1970).
- , and G. W. Roberts, "Kinetics of Thiophene Hydrogenolysis on a Cobalt Molybdate Catalyst," *AIChE J.*, **14**, 159 (1968).
- Schuman, S. C., and H. Shalit, "Hydrodesulfurization," *Catal. Rev.*, **4**, 245 (1970).
- Seshadri, K. S., F. E. Massoth, and L. Petrakas, "Electron Spin Resonance and Microbalance Study of Sulfided Molybdena-Alumina Catalysts," *J. Catal.*, **19**, 95 (1970).
- Sleight, A. W., and B. L. Chamberland, "Transition Metal Molybdates of the Type AMoO_4 ," *Inorg. Chem.*, **7**, 1672 (1968).
- Smith, G. W., and J. A. Ibers, "The Crystal Structure of Cobalt Molybdate, CoMoO_4 ," *Acta Crystallogr.*, **19**, 269 (1965).
- Tomlinson, J. R., R. O. Keeling, Jr., G. T. Rymer, and J. M. Bridges, "Magnetic and Catalytic Studies of Supported Cobalt Catalysts," *Actes du deuxième Congr. Intern. de Catalyse*, pp. 1831-1850, Ed. Technip, Paris (1965).
- van Deemter, J. J., "Trickle Hydrodesulfurization—a Case History," in *Third European Symp. on Chem. Reaction Eng.*, pp. 215-223, Pergamon Press, Oxford (1965).
- van den Berg, J. M., "Structure and Magnetic Susceptibility of CoMo_2S_4 ," *Inorg. Chim. Acta*, **2**, 216 (1968).
- van Reijen, L. L., "Electron Spin Resonance Studies of Pentavalent and Trivalent Chromium," Ph.D. thesis, Technical Univ. Eindhoven, The Netherlands (1964).
- van Swaaij, W. P. M., J. C. Charpentier, and J. Villenmaux, "Residence Time Distribution in the Liquid Phase of Trickle Flow in Packed Columns," *Chem. Eng. Sci.*, **24**, 1083 (1969).
- van Zoonen, D., and C. Th. Douwes, "Effect of Pellet Pore Structure on Catalyst Performance in the Hydrodesulfurization of Straight-Run Gas Oil," *J. Inst. Petrol.*, **49**, 383 (1963).
- Vlugter, J. C., and P. Van't Spijker, "Catalysts for Hydrocracking of Distillates and Residuums," in *Proc. of 8th World Petrol. Congress*, **4**, pp. 159-168, Applied Science, London (1971).
- Voorhoeve, R. J. H., "Electron Spin Resonance Study of Active Centers in Nickel-Tungsten Sulfide Hydrogenation Catalysts," *J. Catal.*, **23**, 236 (1971).
- , and J. C. M. Stuiver, "Kinetics of Hydrogenation on Supported and Bulk Nickel-Tungsten Sulfide Catalysts," *ibid.*, 228 (1971a).
- , "The Mechanisms of Hydrogenation of Cyclohexane and Benzene on Nickel-Tungsten Sulfide Catalysts," *ibid.*, 243 (1971b).
- Voorhoeve, R. J. H., and H. B. M. Wolters, "Tungsten Sulfides obtained by Decomposition of Ammonium Tetrathio-tungstate," *Z. Anorg. Allg. Chem.*, **376**, 165 (1970).
- Weekman, V. W., unpublished comments, Fifth European/Second Intern. Symp. on Chem. Reaction Eng., Amsterdam (1972).
- Wilson, J. A., and A. D. Yoffe, "Transition Metal Dichalcogenides. Discussion and Interpretation of Observed Optical, Electrical and Structural Properties," *Advan. Phys.*, **18**, 193 (1969).

The cooperation of the Research Committee of the AIChE in obtaining this review is acknowledged.